


**Monitoring small reservoirs in
Zimbabwe's Midlands province
using Sentinel-1 SAR and optical
satellite imagery**

MUKETIWA CHITIGA
February 2017

SUPERVISORS:
Dr. Ir. Rogier van der VELDE
Dr. Zoltán VEKERDY



Monitoring small reservoirs in Zimbabwe's Midlands province using Sentinel-1 SAR and optical imagery

MUKETIWA CHITIGA

Enschede, The Netherlands, 19 February, 2018

Thesis submitted to the Faculty of Geo-Information Science and Earth Observation of the University of Twente in partial fulfilment of the requirements for the degree of Master of Science in Geo-information Science and Earth Observation.

Specialization: Water Resources and Environmental Management

SUPERVISORS:

Dr. Ir. Rogier van der VELDE

Dr. Zoltán VEKERDY

THESIS ASSESSMENT BOARD:

Dr. M.W. LUBCZYNSKI (Chair)

Dr Ir.D.C.M. AUGUSTIJN (External Examiner, University of Twente)

Dedicated to a long list of individuals that have made a difference for me in the School of life.

DISCLAIMER

This document describes work undertaken as part of a programme of study at the Faculty of Geo-Information Science and Earth Observation of the University of Twente. All views and opinions expressed therein remain the sole responsibility of the author, and do not necessarily represent those of the Faculty.

ABSTRACT

Small reservoirs represent life and opportunities for many rural communities due to their multiple usages such as watering of gardens, brickmaking, small fisheries, and livestock watering. However, very little information on their surface areas and storage is available in the public domain because. The knowledge base and management is usually limited to localised systems. Earth observation offers opportunities for rapid assessment of the surface areas of these reservoirs and a means to compute storage using other indirect methods. Sentinel-1 Synthetic Aperture Radar (SAR) has the advantages of being weatherproof and can operate day and night therefore it can offer a continuity of datasets as compared to optical sensors however it is hard to interpret. Data availability is no longer an issue like before, because of the European Space Agency (ESA) currently has an open data policy. The purpose of this study was to monitor small reservoirs of different within Zimbabwe using Sentinel-1 SAR, which was not possible before because of the non-availability of operational SAR system. Sentinel-1 SAR images acquired in the interferometric wide (IW) swath mode at an incident angle between 30 and 46 degrees trained on Sentinel-2 and Landsat-8 Modified Normalised Difference Water Index (MNDWI) water body masks were used to extract ArcGIS format polygons. Optimal σ_{VV} and σ_{VH} thresholds were identified to be -18 dB for VV and -22 dB for VH through trial and error. The extracted surface areas were tested against an insitu dataset collected by taking GPS points around the shoreline of the reservoirs using metrics of Relative Mean Absolute Error (RMAE) and Relative Bias. The datasets were highly correlated but gave a low accuracy of 63.1 %, which could be attributed to a difficulty in extracting a reliable dataset due to the presence of vegetation along the shorelines of most of the twenty-one reservoirs surveyed. Other sources of the error could be noise within the SAR images themselves, and the thresholding methods, however there were no major differences between the VV and the VH polarised surface area extractions. Visual inspections of extracted polygons were used to decide on their performance. Overall, the VH polarisation had higher extractions than the VV, which had some inconsistencies and mis classifications. Generally, Sentinel-1 SAR performed much better on relatively larger reservoirs than on small ones leading to possible conclusions that size, location and geometry have an effect on the backscatter signals received and transmitted over a water body. A more rigorous method of determining the threshold and a more improved method of collecting the in-situ data set could help in reducing some of the error. A time series analysis captures the match in surface area dynamics and the seasons of the year. Usage played a role on the smaller reservoirs under intensive usage, however the best performing reservoir is used for irrigation but was extracted more accurately because it has less vegetation along its shoreline.

Key words: Backscatter, Polarisation, Small reservoir, Surface area, Accuracy

ACKNOWLEDGEMENTS

Many thanks to the following:

- My supervisors, Dr R van de Velde and Dr Z Vekerdy for their supervisory efforts in guiding the course of this study even if things got out of hand sometimes (as they should) in the pursuit of knowledge, understanding and skills.
- The whole WREM class of 2018 for their numerous valuable contributions to my studies and social life. These are the people that I spent 18 months in a foreign land with through some good and not so good times. You rocked! Yes, I made 20+ friends and family for life.
- My son Rene accompanied me on the first day of fieldwork and made his contribution by taking pictures but gave up thereafter because of the mud and the effort to walk around the perimeter of a reservoir.
- Promise and Jabula Sibanda accompanied me to four reservoirs and drove me on the bad patch in their truck, much appreciated.
- Khumetsi Nare thank you for the company to Somabula.
- Lyndsey for the airport pickup, persevering to proof read even if she had no idea what I was talking about and the patience to listen to me rant and rave about stuff that goes south from Business development and Sales! You make me smile and proud to be yours.
- Ben Mabenge for the rapid lessons in Global Mapper and a reminder of the great times at ZINWA and thereafter.
- Ochieng' Mc'Okeyo, yes you had to check your name was spelt right. Thank you for all the help my brother from another side of Africa.
- Agbor, Ali, Achimwene, Sylo, Simon and Donald, Samuel.
- I would also want to acknowledge Professor Dominic Mazvimavi for his quick reponse and advice on the use of the Mavimavi et al, 2004 model.
- Dr T Sawunyama for responding to questions regarding his model.

Indeed, I came to ITC with no fellow countryman or woman to relate to, but ITC shaped my international relations. I made of friends and acquaintances across, races, continents and religions since this journey began. I have learnt and unlearnt many things from these same people. Some I may not mention by name herein but I will give my thanks and appreciation for their input.

Thank you
Dank je wel
Mucha gracias
Kealebuwa
Asante sana

TABLE OF CONTENTS

1.	Introduction.....	1
1.1.	Background.....	1
1.2.	Academic context.....	2
1.3.	Research objectives and questions.....	3
1.4.	General research methods.....	3
1.5.	Thesis Structure.....	4
2.	Literature review.....	5
2.1.	Defining a small inland reservoir.....	5
2.2.	Importance of small reservoirs.....	5
2.3.	Synthetic Aperture Radar and water body extraction.....	6
2.4.	Remote sensing from optical imagery.....	7
2.5.	Masking water bodies using optical satellite images.....	7
2.6.	Small reservoir capacity estimates.....	8
3.1.	Midlands province.....	10
3.2.	In-situ data set.....	11
3.3.	Procedure of recording vertices.....	13
3.4.	Digitising the in-situ dataset.....	14
4.	Satellite Imagery.....	16
4.1.	Sentinel-1 SAR.....	16
4.2.	Delineation of water reservoirs using Sentinel-1 SAR.....	18
4.3.	Landsat 8 OLI.....	18
4.4.	Sentinel-2 MSI.....	20
5.	Methods.....	23
5.1.	Masking of water bodies using optical imagery.....	23
5.2.	Accuracy assessment and threshold determination.....	26
5.3.	Sentinel-1 SAR time series.....	26
5.4.	Translating Area to Volume.....	27
6.	Results & Discussion.....	28
6.1.	Identifying a suitable threshold.....	28
6.6.	Time series.....	32
6.7.	Accuracy of retrievals.....	33
6.8.	From surface area to storage.....	35
7.	Conclusions, Limitations & Recommendations.....	36
7.1.	Conclusions.....	36
7.2.	Limitations.....	37
7.3.	Recommendations.....	37

LIST OF FIGURES

Figure 1-1. Scheme of the processes followed in the course of this research.....	4
Figure 3-1. The Midlands province and the location of the study area.....	10
Figure 3-2. Location of all the reservoirs that formed the in-situ dataset.....	11
Figure 3-3. Images of selected reservoirs during in-situ data collection.....	12
Figure 3-4. Extraction of the shoreline of the Somkhaya reservoir (12/09/2017)	14
Figure 4-1. Sentinel-1 SAR image in RGB presentation.....	18
Figure 4-2. Landsat-8 OLI image in RGB presentation	20
Figure 4-3. Sentinel-2 MSI image in RGB representation.....	22
Figure 5-1. Masking of water bodies on a Landsat-8 image.....	24
Figure 5-2. Masking of water bodies on a Sentinel-2 image.....	25
Figure 6-1. Analysis of error on the Landsat-8 image, 20170905 image	29
Figure 6-2. Analysis of error on the Sentinel-2, 20170909 image.....	29
Figure 6-3. Finding the optimal threshold on Ngwena using Sentinel-1 SAR and Sentinel-2.....	30
Figure 6-4. Finding the optimal threshold on Ngwena using Sentinel-1 SAR on Landsat-8.....	30
Figure 6-5. Finding the optimal threshold on Mutorahuku using Sentinel-1SAR on Sentinel-2	31
Figure 6-6. Finding the optimal threshold on Mutorahuku using Sentinel-1 SAR on Landsat-8.....	31
Figure 6-7. Time series of extracted surface area from selected reservoirs	32
Figure 6-8. Surface area extractions on the Ngwena reservoir using different datasets	33
Figure 6-9. Comparison of relative errors from the different datasets.....	34
Figure 6-10. Fluctuations in storage in selected reservoirs	35

LIST OF TABLES

Figure 1-1. Scheme of the processes followed in the course of this research	4
Table 2-1. List of International and Zimbabwean definitions of a small reservoir	5
Table 2-2. Definition of SAR Radar frequency bands.....	6
Table 2-3. Storage-Area relationships developed in Zimbabwe	9
Table 3-1. Full list of reservoirs that formed the in-situ dataset.....	13
Table 3-2. List of reservoirs dropped from further analysis.....	15
Table 3.3. Reservoir surface area calculation for the selected reservoirs.....	15
Table 4-1. Characteristics of Sentinel-1 SAR sensor.....	16
Table 4-2. Final GeoTIFF images used for the study.....	17
Table 4-3. Rearranged Landsat-8 OLI spectral bands.....	19
Table 4-4. List of cloud free Landsat 8 OLI images selected for the study	19
Table 4-5. Rearrangement of Sentinel-2 spectral bands according to a common resolution.....	21
Table 4-6. List of cloud free Sentinel-2 MSI images available for the study area	21
Table 5-1. Calculated water indices, their formulae and applicability to each sensor.....	23
Table 5-2. Thresholds applied to the different images	25
Table 5-3. Matching of September 2017 remote sensing datasets for calibration and accuracy assessment.....	26
Table 5-4. Thresholds applied on the optical and SAR images	27
Table 6-1. Error propagation on Sentinel-1 SAR trained on Landsat- 8.....	28
Table 6.2. Error propagation on Sentinel-1 SAR image trained on Sentinel-2	28
Table 6-3 Surface area retrievals from the different datasets used in the study	34
Table 6-4. Average relative absolute errors and inferred accuracy of each dataset.....	35
Appendix 1. Typical retrievable metadata file for Sentinel-2 subsets from Global mapper.....	46
Appendix 2a. List of all reservoirs surveyed for the study.....	47
Appendix 2b. Further information on usage and location of small reservoirs used in the study.....	Error!

Bookmark not defined.

1. INTRODUCTION

1.1. Background

Water is indispensable and represents physical, social, spiritual, political, economic and environmental realms in its cyclic nature (Juuti & Katko, 2004). It has helped generations of mankind shape their livelihoods locations of its abundance and ease of portability (Strang, 2004, Sedlak, 2014). Across history, civilisations have acquired skills to manage water, such as storage, conveyance, diversions, and demand management because it renews itself. Despite it being renewable, water shortages are on the increase in many regions of the world (Eliasson, 2014). This is mainly due the pressures exerted by increasing complexity in competitive water related demands and increasing global populations which raise the potential of a global water crisis (Postel, 2006). Alarming statistics from United Nations (2017) indicate that 40 % of the global population is already affected by water scarcity with approximately 1.7 billion people currently living in river basins where water use exceeds replenishment and this is a characteristic of most arid climates.

The majority of semi-arid zones in the world are located in developing countries (Finch, 1997). These areas are usually characterised by erratic seasonal rainfall patterns causing floods and droughts (Rodrigues et al, 2012). However, damming of rivers and streams to create reservoirs for storing excess water for use during dry months or flood control is a coping mechanism. The terms *dam* and *reservoir*, are often used interchangeably, but for consistency, *reservoir* will be used in this study. Classification of man-made reservoirs is normally based on storage capacity, dam wall height and material used in construction. Substantial information on large reservoirs is usually available from websites, water authorities and databases (Lehner et al., 2011; Lehner & Döll, 2004; Liebe, van de Giesen, Andreini, Walter, & Steenhuis, 2009) while that of small reservoirs is sparse or unavailable.

Zimbabwe is a semi-arid country located in Southern Africa. It has distinct wet and dry seasons with rainfall between November and March (Unganai & Mason, 2002). Excess water is stored in surface water reservoirs that were constructed in most parts of the country, however other areas rely on groundwater especially in the dry season. The Zimbabwe National Water Authority (ZINWA) is mandated by law to manage all water resources in Zimbabwe, but we have instances where water bodies are operated by cities, private entities and other public institutions as well (Zimbabwe Parliament, 1998). Small reservoirs make up a significant proportion of the total number of reservoirs in Zimbabwe. However, crucial information such as storage capacities, spatial distribution and water quality is not readily available which is quite common in many developing countries (Rodrigues et al, 2012). Most of these small reservoirs have not been accepted as important components of the of river basin hydrology and catchment management in general (Sawunyama et al, 2006), yet they provide value to many communities due to their multiple uses.

Globally and even within Zimbabwe, varying definitions of what constitutes a small reservoir exist. These definitions do not necessarily concur with each other (Payen, Faurès, & Vallée, 2012) because classification is based not only on size but a combination of criteria. International bodies such as the international Commission on Large Dams (ICOLD), World Bank and the Food and Agricultural Organization (FAO) have their own different combinations of standardised criterias. There seems to be a wide acceptance that a capacity $>1\ 000\ 000\ m^3$ defines a small reservoir (Pawson et al, 2010; Payen et al., 2012). However, reservoirs as small as 0.1 ha in surface area do occur which therefore makes it difficult to place them within context.

1.2. Academic context

The Zimbabwe National Water Authority (ZINWA) is a statutory body created through the Zimbabwe National Water Authority Act, (Chapter 20:25) to enforce the Water Act (ZINWA, 2016). Its mandate by law is to manage all water resources within Zimbabwe at national, catchment and sub-catchment scales. The latest Zimbabwe National Water Policy document acknowledges the existence of unconfirmed figures of reservoirs of varying sizes within rural or farming areas (Government of Zimbabwe, 2013). However, the information is limited to local knowledge about the reservoir (Chimowa & Nugent, 1988). Important information that helps in water management such as the storage capacities and their usage is either poorly represented or unavailable (Mugabe et al., 2003). The policy also stipulates that Rural District councils (RDC), will manage small reservoirs in Zimbabwe, but is not explicit on how they should play their role to achieve policy objectives. It is also crucial to note that abstraction from most small reservoirs is classified as primary purposes and no therefore no payment for water is required according to the Water Act (Zimbabwe Parliament, 1998). Changes in land tenure systems have resulted in more farm-based reservoirs changing ownership from private protected state to communal property. Storage capacity and planning information related to the usage of these reservoirs was lost in the transition. Most small reservoirs have aged, and most have silted up due to lack of clear protection, management and maintenance.. The risk associated with siltation (Chitata, et al., 2014), washing away (Rukuni, 2006) or drying up before the end of the dry season is unknown. Management has for the most part been the responsibility of communities who may not have adequate capacity to allocate, optimise and enforce the use of scarce water resources, especially during dry months.

The lack of information on the current storage or water levels of small surface water reservoirs is twofold: i) delineating and calculating the surface area occupied by a reservoir at a specific time and ii) estimation of the volume of water within that reservoir at that specified time. This can be addressed in-situ, via earth observations or an integration of the two methods. Field measurements are often costly and time consuming (Lu et al, 2013; Rodrigues et al., 2012), while remote sensing methods can offer rapid and updated datasets at regular time intervals. The different earth observation techniques have their advantages and disadvantages over each other. For instance, optical remote sensing is affected by cloud coverage, while that from the microwave portion of the electromagnetic spectrum has all weather capability (Lillesand, Kiefer, & Chipman, 2004), but are more difficult to interpret. Within Africa, work was successfully carried out to identify and retrieve surface areas of small inland water bodies using mainly optical imagery. Liebe et al., (2009), Meigh, (1995), and Sawunyama et al.,(2006) used Landsat imagery in West Africa and Southern Africa respectively. Other optical datasets such as TERRA/MODIS were used in West Africa (Magome, Ishidaira, & Takeuchi, 2003) for the same purposes. Synthetic Aperture Radar (SAR) datasets from the Japanese Earth Resource SAR (JER-1/SAR), Environmental Satellite Advanced SAR (ENVISAT ASAR) and COntellation of small Satellites for the Mediterranean basin Observation (COSMO-SkyMed) satellites were used by (Amitrano, Martino, Iodice, Riccio, & Ruello, 2017; Eilander, 2013; Magome et al., 2003) respectively to extract water body surfaces in Burkina Faso and Ghana.

Computing the capacity or volume of a reservoir solely using remote sensing is currently not possible. Storage capacities are typically determined from bathymetry exercises, which are time consuming and expensive, however there is an established relationship that exists between surface area, depth and volume of a small reservoir (Liebe, (2002). Additionally, Sayl et al, (2017), elaborated that there is a correlation between the geometry of a reservoir, its surrounding topography and its volume. Regression can then be used to produce individual functions which can be averaged to give a mean basin-specific rating curve (Mitchell, 1976; Rukuni, 2006) which are then used to translate area to volume. This is achieved on the basis that reservoirs located in areas of the same physiographic structure have closely related geometry and depths (Grin, 2014). Other studies (Ran & Lu, 2012; Rodrigues et al., 2012; Sayl et al., 2017) developed area-capacity

functions for small reservoirs in the Yellow, Preto and Euphrates basins respectively using the same methods.

The European Space Agency (ESA) supervises the development of the Sentinel satellites, of which Sentinel-1 SAR is a component. It comprises a pair (Sentinel-1A and B) of near-polar sun-synchronous orbiting satellites, launched on 3 and April of 2014 and 2016 respectively (Copernicus, 2018; Minchella, 2016). The Sentinel-1 C-band imaging SAR is responsive to land surface roughness, near surface soil moisture and open water bodies. It potentially delivers images in dual polarizations of VV+VH or HH+HV (Potin et al, 2016). Images are freely downloadable from the Sentinels Science data hub (<https://scihub.copernicus.eu/dhus/#/home>) and other free SAR data platforms such as the Alaska Satellite Facility (<https://vertex.daac.asf.alaska.edu/>). SAR has the major advantages of day and night operation and the ability to penetrate through atmospheric debris and clouds resulting in all acquisitions being useful unlike optical sensors. As been discussed in the previous section, SAR imagery has been used before for retrieval of surface areas of small reservoirs. Prior to the open data policy from 2010 monitoring of small reservoirs using SAR imagery was not possible because images were not available on an operational basis. The launch of Sentinel-1 SAR coupled with its high accuracy and the open data policy opened up new opportunities to exploit its capabilities to frequently monitor small reservoirs (Amitrano et al., 2014).

1.3. Research objectives and questions

The main objective of this study is to estimate the dynamics of the surface areas and compute the storage of small multi-purpose reservoirs located in the Midlands Province of Zimbabwe using Sentinel-1 SAR in combination with the optical imagery (Sentinel-2 or Landsat-8). The following specific objectives were formulated for achieving the main objective:

- i) Design and perform a ground truth sampling data set that enables validation of the EO-based surface area estimates for a number of reservoirs varying in size and usage (e.g. community, smallholder farmers, and farming).
- ii) Develop a method for delineation of the boundary of small reservoirs and applying the high temporal resolution and dual-polarization capability of Sentinel-1 SAR data in combination with optical imagery (Sentinel-2 MultiSpectral Imager (MSI) or Landsat-8 Operational Land Imager (OLI)).
- iii) Validate the EO-based surface area estimates using field data and determine the performance of EO-based methods.
- iv) Analyze the temporal fluctuations in the storage of various type of small reservoirs.

Based on the research objectives, the following research questions were formulated:

- i) What are the challenges in ground sampling?
- ii) Is Sentinel-1 SAR an effective data source for retrieving surface area of small reservoirs?
- iii) What is the impact of reservoir size on the accuracy of the retrieval methodology?
- iv) How does storage fluctuate in different sizes of reservoirs over time and how is it related to usage?

1.4. General research methods

The research had two components, fieldwork and remote sensing. Fieldwork was carried out from 9-21 September 2017 to acquire the in-situ dataset. It involved the collection, processing and computation of the surface areas of 21 small reservoirs of varying sizes and produce ArcGIS format polygons of reservoirs at the time of satellite overpass. Remote sensing datasets covering the study area were downloaded from their

respective archives, pre-processed and surface areas of the same reservoirs extracted for comparison with the field data acquired in September 2017. The remotely sensed datasets are, Sentinel-1 SAR, Sentinel-2 MSI and Landsat-8 OLI. Figure 1 shows a scheme of the methods adopted in this research.

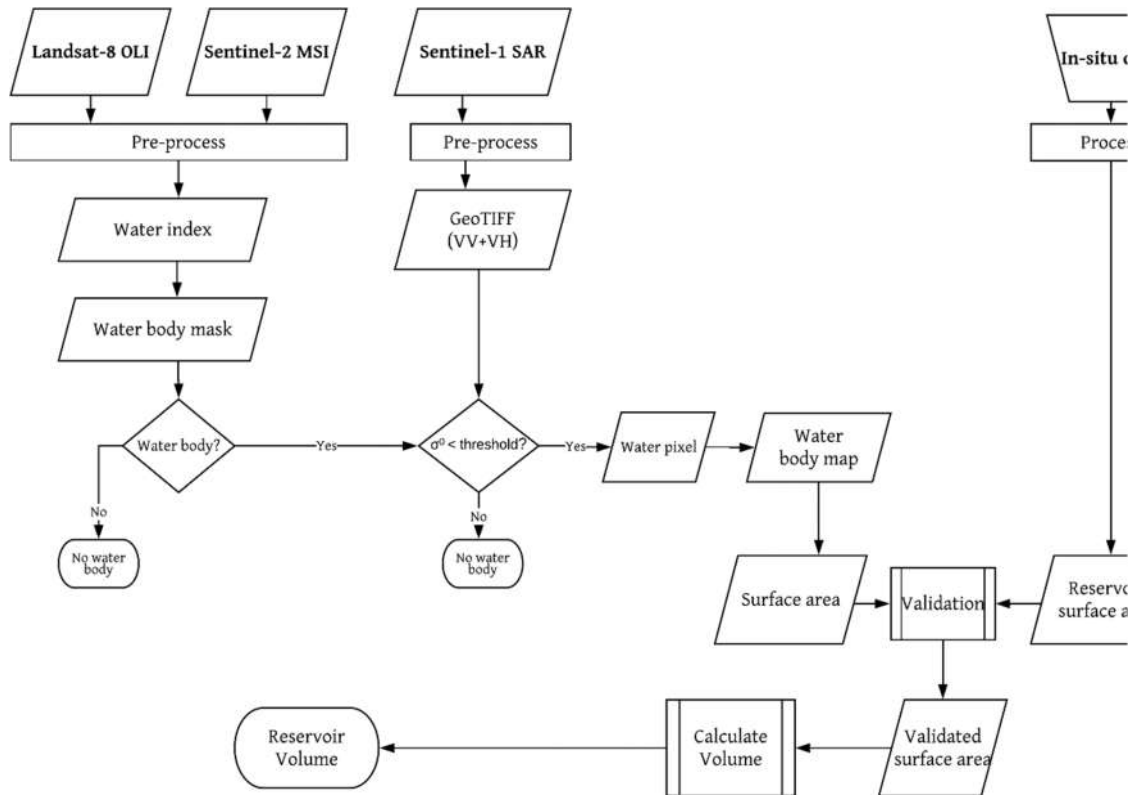


Figure 1-1. Scheme of the processes followed in the course of this research

1.5. Thesis Structure

The thesis is outlined in seven sections. Chapter 1 introduces the subject, the academic context, objectives and formulate research questions. Chapter 2 gives an overview of a literature search on the subject. Chapter 3 describes the study area and the in-situ dataset. Chapter 4 discusses the remotely sensed datasets and their pre-processing. Chapter 5 describes the methods used in the analysis in detail. Chapter 6 presents and discusses the results of the different analyses. Chapter 7 presents the conclusions, limitations and recommendations from this research. References and appendices are presented at the end of the document.

2. LITERATURE REVIEW

2.1. Defining a small inland reservoir

Small water bodies are various types of water storage systems that include ponds, pools, weirs, canals and lakes that occur everywhere. This description is inadequate to describe a reservoir, therefore the input of regulation, control or management of water helps to align the definition to explicitly refer to a reservoir (Ignatius, 2009). In simple terms, the dam refers to a structure constructed to stop the flow of water across a stream in order to raise the level of water and create an impoundment of water behind it, which becomes the reservoir. Classification of a typical water storage reservoir is usually based on purpose, construction material used, wall height and capacity (SANCOLD, 2017). For the purposes of clarifying the ambiguity on what constitutes a small reservoir, different definitions of a small reservoir are shown in Table 2.1.

Table 2-1. List of International and Zimbabwean definitions of a small reservoir

Organisation	Variable	Reference
	Dam wall height Capacity	
WCD ⁺⁺	<15 m	<1 000 000m ³ (WCD, 2000)
USA [#]	≤ 10.6	3 700 440 m ³ (Nebraska Department of Natural Resources, 2013)
ICOLD [*]	<5-15m	<3 000 000 m ³ (FAO, 2007)
IWMI [~]	<7.5m	≤1 000 000 m ³ (Venot & Hirvonen, 2013)
-		5 00 000 - 1 000 000 m ³ Zimbabwe Water Act (1998)
DWR ⁺	<8 m	< 1 000 000 m ³ (Mazvimazvi et al, 2004)
ZINWA ⁺	<10m	1 000 000 m ³ Muyambo (2000)

⁺Zimbabwe Department of Water Resources ^{*}International commission on large dams, ^{##}Zimbabwe National Water Authority

⁺⁺World Commission on Dams, [#]United States of America [~]International Water Management Institute

None of the descriptions above suits the perceptions of most small reservoirs as adopted in this research. The closest definition is the one given by Eilander (2013), which however falls short in fully describing the majority of small reservoirs, which are realistically between 0.1 and 30 ha in surface area.

2.2. Importance of small reservoirs

Studies carried out in the Limpopo basin under the Small Reservoirs Project (SRP) framework (Andreini et al., 2009), informed on the socio-economic importance of small reservoirs. (Mufute, 2007; Munamati & Senzanje, 2015; Sawunyama et al., 2006). However, sustainable utilisation and management of small reservoirs in other areas of the country is seriously affected by lack of current data (Chitata et al., 2014). The role of small reservoirs within the overall hydrological systems is still largely undervalued by the focus on the bigger reservoirs which supposedly provide 'higher returns' to society (Downing, 2010). In terms of density, distribution and functionality, small reservoirs combined, meet local needs for many communities (Simmers, 1999) and have a lesser ecological footprint on the environment compared to large reservoirs (Hughes et al, 2010). There is mention, in Dalu, Clegg, & Nhiwatiwa (2013), of the existence of between 50 to 100000 small reservoirs in the Southern African Development Community (SADC) region. Approximately 14000 of these were located in Zimbabwe according to Marshall & Maes, (1994). Chimowa & Nugent (1988) also cited approximately 9800 entries while Senzanje et al, (2008), and Senzanje & Chimbari (2002, unpublished), also

mention approximately 10000 reservoirs. However, there is no existing public registry to support these facts as is the case in South Africa, Lesotho and Swaziland (Mantel et al, 2017).

Traditionally, water usage has been monitored using existing water measuring devices installed on water storage reservoirs usually during construction. However, within Africa in general, in-situ monitoring has financial, institutional and spatial limitations (Ballatore et al, 2014). Additionally, reservoir capacities are not static and change with aging of the reservoir and increasing water demand. Water measuring infrastructure and devices have a tendency to either malfunction or become obsolete and have prohibitive replacement costs (Duy, 2015) Access may be hindered by topography, vegetation regrowth, conflicts, armed conflicts and natural disasters. In-situ systems for small reservoirs are very limited within developing nations which makes the use of earth observation technology an available option to fill the gap (Avisse, Tilmant, François Müller, & Zhang, 2017; Ballatore et al., 2014) by providing reasonable estimates for monitoring purposes, usually in combination with other available methods to maintain continuity in data collection.

2.3. Synthetic Aperture Radar and water body extraction

The term Radio Detection and Ranging (RaDAR) refers to active systems, which operate from the microwave region of the electromagnetic spectrum within wavelengths of 1mm-1m (Awange & Kyalo Kiema, 2013). It records the features of objects on the earth's surface just like optical systems but retrieves different detail (Lillesand, Kieffer, & Chipman, 2004). Other than weather independence, RaDAR possesses day and night capabilities and operate at a prescribed wavelength, and polarisation (Campbell & Wynne, 2011)(Campbell & Wynne, 2011). Historically, Seasat was the first civilian space-borne imaging RaDAR satellite to launch a SAR sensor in 1978 and was primarily designed for oceanic studies (Natural Resources Canada, 2017). Notable satellite missions that followed the launch of the Seasat are outlined (ESA, 2017b; Madry, 2013):

- i) ENVISAT ASAR
- ii) RADARSAT
- iii) ERS1 (1991-2000. ESA's first EO satellite and long term satellite radar imager).
- iv) Shuttle Radar Mission Topography Mission (SRTM) (From 2000 and produced a near global high resolution interferometric DEM which had the highest resolution for that time).
- v) Tandem-X (2010-2014).
- vi) Sentinel-1 (The current mission of the ESA supporting SAR data).

SAR is an imaging side-looking RaDAR system that uses the Doppler shift principle from the platform's forward motion for improving spatial and azimuth resolution by simulating a larger antenna from a smaller one (Chan & Koo, 2008). Very high-resolution commercial SAR systems such as Cosmo Sky-Med, TerraSAR-X and Radarsat can achieve around 3 m, while Sentinel-1 provides 10 m. Table 2.2 shows the SAR frequency bands and satellites that operate in them.

Table 2-2. Definition of SAR Radar frequency bands

SAR band	Frequency (GHz)	Wavelength (cm)	Example satellite
P	0.230 -1	130 - 30	BIOMASS
L	1.0-2.0	30 - 15	Seasat, SIR-A & B, ALOS-1 & 2, JER-1
S	2.0-4.0	15 - 7.5	Immarsat, ALMAZ-1, HJ-1-C
C	4.0-8.0	7.5 - 3.75	ERS-1 & 2, STRM, ENVISAT, Sentinel-1, Radarsat-1 &- 2
X	8.0-12.5	3.75 - 2.40	SRTM, TerraSAR-X, TanDEM-X, COSMO-SkyMed

Adapted from (Lillesand et al., 2004,ESA, 2017a)

The satellite transmits microwave pulses to the earth's surface, which is then returned to the satellite sensor as backscatter to create an image (ESA, 2009). Interaction with different material on the ground is based on the surface roughness and the three scattering mechanisms, i.e. specular, diffuse and double bounce (Woodhouse, 2006). SAR allows us to receive and send signals based on the different combinations of the vertical and horizontal polarisations however it is sensitive to surface roughness resulting in possible misclassifications (Lavender & Lavender, 2016). Specular or mirror-like reflection is dominant on calm water surfaces and the low signal received at the sensor produces dark tones on the image (Woodhouse, 2006). Diffuse scattering becomes more dominant on rough surfaces (vegetation and soil) and gives an intermediate amount of backscatter (Natural Resources Canada, 2017). The information retrieved by SAR data find applicability in many applications, such as change detection in water resources, flood monitoring and disaster management.

In SAR imagery, various supervised and unsupervised classification methods for separating water bodies from land exist. However, histogram thresholding is the most common. It consists of establishing a value *less than* or *equal* to which pixel values are selected and classifying everything else as non-water to achieve a separation (Bolanos et al, 2016). Researchers have used automatic extraction threshold selection methods, such as the Otsu algorithm resulting in an image with two classes (Li & Wang, 2017). Variations of the Otsu algorithm such as, the Valley-Emphasis method (Duy, 2015), and the box classifier by Yang & Zmuda, (1998). In addition, tools such as the Forest non-Forest Class Extraction (FnFCE) were developed in Canada for Radarsat 1 imagery (Short, Brisco, & Landry, 2011). The growing Bayesian classifier methodologies ((Amitrano et al., 2014; Eilander et al., 2014) and application of neural networks (Pham-Duc, Prigent, & Aires, 2017) were used to achieve separation.

2.4. Remote sensing from optical imagery

The Landsat programme became the first moderate resolution civilian remote sensing system in 1970 (Madry, 2013). It has produced the longest global coverage of satellite data series, which has helped in the development of several scientific and commercial applications. On the other hand, the French Satellite Pour l'Observation de la Terre (SPOT) program pioneered commercial satellite imagery with an impressive ground resolution of 10 m from 1986 (Chevrel, Courtois, & Weill, 1981). Several new satellites such as IKONOS, GeoEye, and Quickbird joined the space fleet thereafter. Currently, more than 30 countries worldwide which operate different categories of remote sensing instruments which offer various types of products of very high (< 5 m), high (5-30-m), medium (30-100 m) and low (250-1,000 m) spatial resolution (Stanniland & Curtin, 2013). Within the developing world, South Africa, Ghana, Nigeria, Brazil and India currently operate space programs.

The use of remote sensing has become one of the most exciting and important methods used in monitoring of the Earth's surface including surface water bodies (Haibo et al, 2011). It offers rapid and consistent methods of identifying and monitoring dynamics within water bodies (Zhai et al., 2015). The open data policies of space agencies such as NASA and ESA have assured the availability of free satellite datasets, which can also be manipulated using open source software such as QGIS, SNAP or ILWIS with the requisite skills.

2.5. Masking water bodies using optical satellite images

Water indices enhance the electromagnetic signal for specified pixels using the visible, near-infrared (NIR), mid-infrared (MIR) and the shortwave infrared (SWIR) bands (Sisay, 2016). They are simple band math ratios using the difference and the sums of reflectance in the chosen bands. There are four categories of methods used in the extraction of water bodies from satellite imagery, i.e. thematic classification, linear unmixing, and two-band spectral indices (Feyisa, Meilby, Fensholt, & Proud, 2014). However, the two-band spectral indices method is the most popular and was used to develop water-sensitive indices which are: i) Normalised Difference Vegetation Index (NDVI), (Rouse, Hass, Schell, & Deering, 1973), ii) Normalised Difference

Water Index (NDWI) (McFeeters, 1996) and a Modified Normalised Difference Water Index (MNDWI), (Xu, 2006).

Notably, the majority of the indices were developed from Landsat products such as Landsat Thematic Mapper and Enhanced Thematic Mapper. Newer documented indices include: SWI (simple water index), (Malahlela, 2016), AWEI (Automated Water Extraction Index), Feyisa et al, 2014), NWI (New water index), (Haibo, Zongmin, Hongling, & Yu, 2011). Additionally, water bodies were mapped at different scales such as global (Downing, 2010), regional (Scholz, 2015) and localised, (Donchyts et al, 2016). Some researchers such as Acharya et al, (2017) blend these indices while others chose to apply indexing in specialised areas such as cryospheric lakes (Jawak & Luis, 2015; Jawak et al 2015).

To give more detail on the classic indices, it is worthy to mention that NDVI was the basis of the development of the common water indices. It was developed by (Rouse et al., 1973) for detecting qualitative aspects in vegetation but was found to be a useful water mask as well (La, Del, & Hamsom, 1987). It uses the difference between strongly reflected and the absorbed NIR and Red light in water (Equation 2.1). Water bodies give very low positive or even slightly negative NDVI values, which normally range between -1 and +1.

$$NDVI = (NIR - Red)/(NIR + Red) \quad (2.1)$$

The NDWI has two versions, one related to vegetation (Gao, 1996) and the other that applies to open water (McFeeters, 1996). It was developed to take advantage of the maximum reflectance in the green, while minimizing the low reflectance of the NIR bands by water bodies (Rokni et al, 2014). The result is a single band mask with positive values signifying water and negative values for non-water features. NDWI (Equation 2.2) has been used widely for water body remote sensing (Yang et al, 2017, Elshabi et al, 2016; Gautam et al, 2015; Jawak & Luis, 2015; Li et al., 2013) but has been criticised for overestimating the sizes of water bodies and failing to discriminate between urban areas and water bodies (Du et al., 2016).

$$NDWI = (Green - NIR)/(Green + NIR) \quad (2.2)$$

A modification of the NDWI was developed by replacing the NIR with the SWIR band and the fact that water absorbs energy at NIR and SWIR wavelengths (Equation 2.3). Modified NDWI (MNDWI) was found to have a remarkable improvement on the shortcomings of the NDWI because it enhances open water bodies while suppressing signals from built-up areas, soil and vegetation (Xu, 2006). The major advantages of using the MNDWI spectral index is that it consistent (Murwira et al, 2014), however it is affected by shadows near mountains or hilly terrain. Generally, MNDWI values > 0 indicate water while those < 0 imply all other feature classes.

$$MNDWI = (Green - SWIR1)/(Green + SWIR1) \quad (2.3)$$

2.6. Small reservoir capacity estimates

Reservoir capacity refers to the maximum amount of water that can be stored in a given reservoir. It is primarily derived from preliminary hydrographic surveys, design reports and measurement of topographic maps with electronic planimeters (Ran & Lu, 2012). Loss of capacity in existing inland surface water reservoirs occurs due to natural or accelerated sediment deposition related to rainstorms and land use practises (Chitata et al., 2014). Periodic bathymetric should be carried out using acoustic instruments mounted on boats to create contour surfaces from the bottom to the top of the lake. The resulting data can be loaded into GIS-based software such as Surfer, Global mapper or ArcGIS for analysis and storage computation based on the geometry of the reservoir. Sawunyama (2005) documented some simple methods for computing the capacity of a small reservoir by measuring the throwback, maximum width and maximum

depth using a distance measuring devices and a graduated depth-measuring probe. Measurements of the throwback and the width can be measured from satellite images or Google Earth. Hudson, (1998), developed the following formula for rapid estimation of reservoir capacities based on the geometry of the reservoir (Equation 2.4)

$$C = \frac{DWT}{6} \quad (2.4)$$

Where: C =Reservoir capacity (m³)

D = the maximum water depth m)

W = the width of water surface (m)

T= the maximum “throwback” from the spillway crest level (m)

Studies carried out to develop methods of translating area to a volume, such as The Small Reservoirs Project (<http://www.smallreservoirs.org/>), developed methods that were applied to small reservoirs that do not have very deep valley cross sections volume. Studies developed relationships of the format in Equation (2.5) and three area capacity relationships developed in different basins within Zimbabwe in 1976, 2004 and 2005 are shown in Table 3.

$$V = kA^y \quad (2.5)$$

Where V = Storage/Volume (m³)

k = basin derived coefficient

A = Surface area (m²)

y = basin derived exponent

Table 2-3. Storage-Area relationships developed in Zimbabwe

Basin	Units				Reference
	Coefficient <i>k</i>	Exponent <i>y</i>	Area	Capacity	
National	2.646	1.5	Ha	10 ³ m ³	(Mitchell, 1976)
Mzingwane	0.023083	1.3272	m ²	m ³	(Sawunyama et al., 2006)
National	7.2	0.77	m ²	10 ³ m ³	(Mazvimazvi et al., 2004)

Although these capacity-area functions were developed using different techniques, times and purposes, there is a reasonable agreement about the possibility of extrapolation to other regions especially within Africa (Grin, 2014; Liebe, 2002). Additionally, geo-morphologically similar regions have almost similar constants and coefficients, however caution is necessary when using these models (Annor et al., 2009; Ran & Lu, 2012) unless they go through rigorous testing and validation. There is a risk associated with using methods developed for another area because of uncertainties related to the variations in shapes and sizes of reservoirs (Sawunyama, 2013).

3.1. Midlands province

The study area is located within the Midlands Province of Zimbabwe within the administrative districts of Gweru and Shurugwi (Figure 3.1). Gweru is the provincial capital and is Zimbabwe's third largest City, which is located in the centre of the country. The Midlands Province is located in Agro-ecological zoning III (Vincent and Thomas in 1960), although a review has been proposed based on climatic changes (Mugandani et al, 2012). The Province normally receives between 550 and 750 mm of rainfall per annum. The majority of the Midlands province is semi-arid to arid with relatively flat and homogenous topography except for the mountainous landscape surrounding the great dyke in Shurugwi District, which has average elevations of 1400 m above sea level.

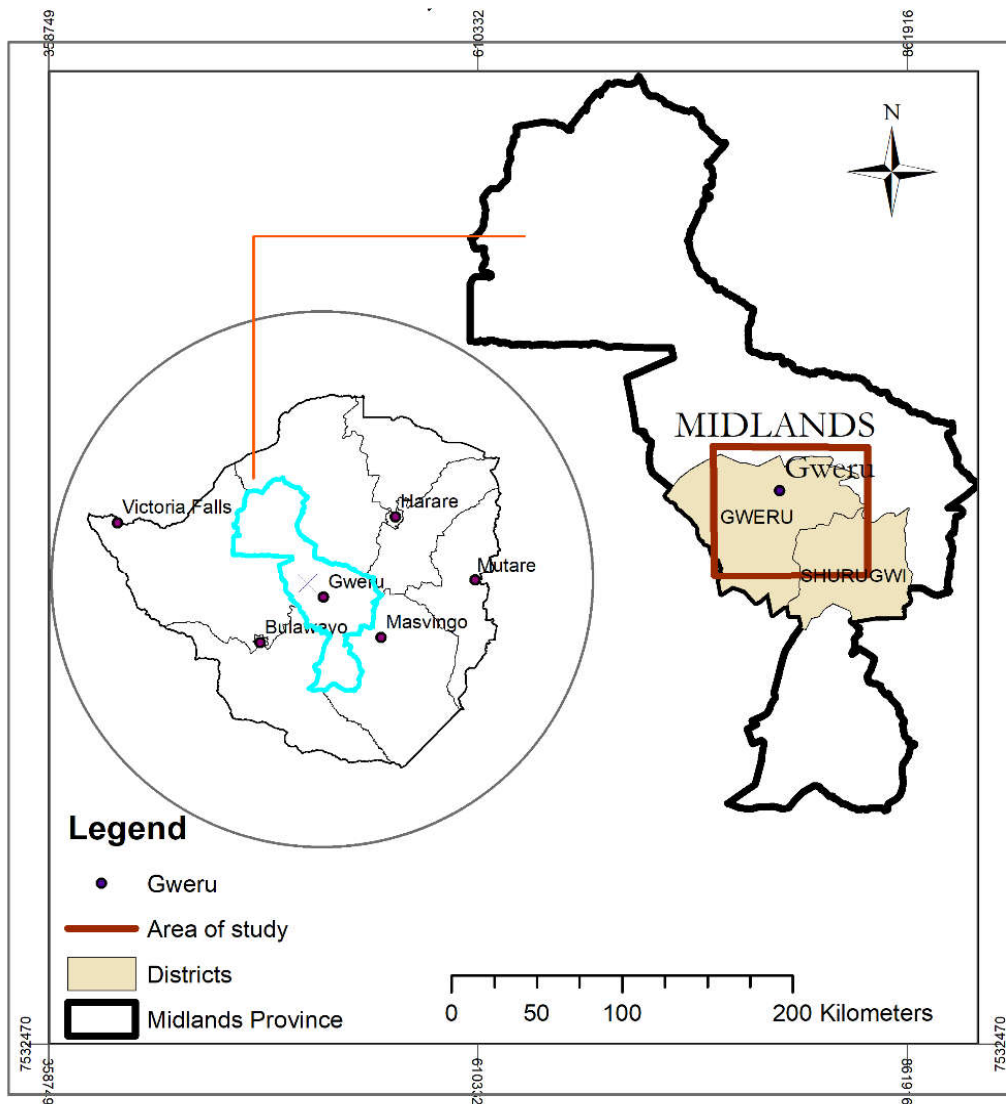


Figure 3-1. The Midlands province and the location of the study area

Small perennial streams in mountainous regions do occur within Shurugwi, Zvishavane and Chiwundura districts. The City of Gweru itself is generally located at the tail ends of three distinct ZINWA catchments of Gwaii, Runde and Sanyati flowing in different directions. Within the Midlands Province, there is a substantial number of reservoirs ranging from < 0.5 to approximately 60 ha in surface area, which are mainly used for water supply, irrigation, mining, fisheries or livestock watering. Information on the number of small reservoirs in the Midlands is presently limited to localised knowledge or private databases, but are expected to be in their thousands. Information on the ground is rather fragmented, but suggest that reservoirs were mainly constructed pre and post-independence in 1980's. The smallest administrative unit in Zimbabwe is a ward and the Shurugwi and Gweru districts have 10 and 12 wards each. Senzanje and Chimbari (2002, unpublished) reported that a deliberate policy meant to provide at least a reservoir for each village in the ward to address water needs was the driver to the construction of most small earth and concrete reservoirs found in Zimbabwe.

Ungauged reservoirs within a radius of 60 km of Gweru located Runde, Gwaii or Sanyati catchments were identified from Google Earth. Twenty-one of the reservoirs of varying sizes were chosen for the study. Figure 3-2 shows the location of the study area.

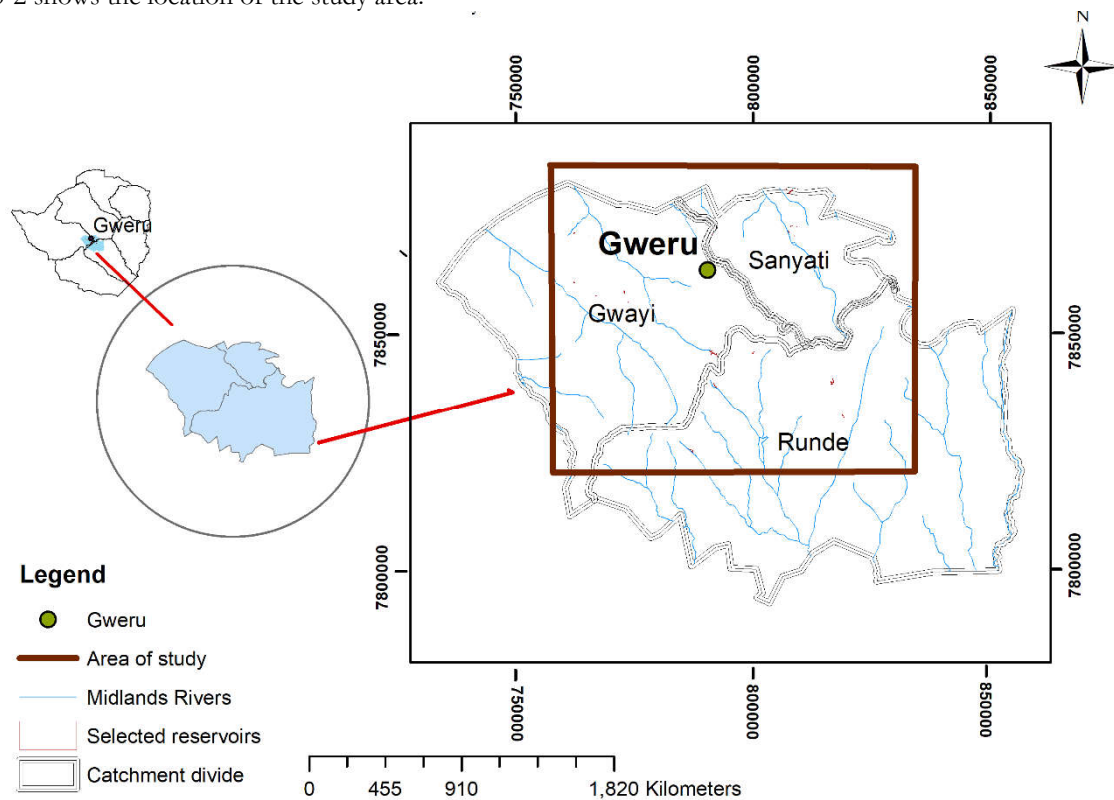
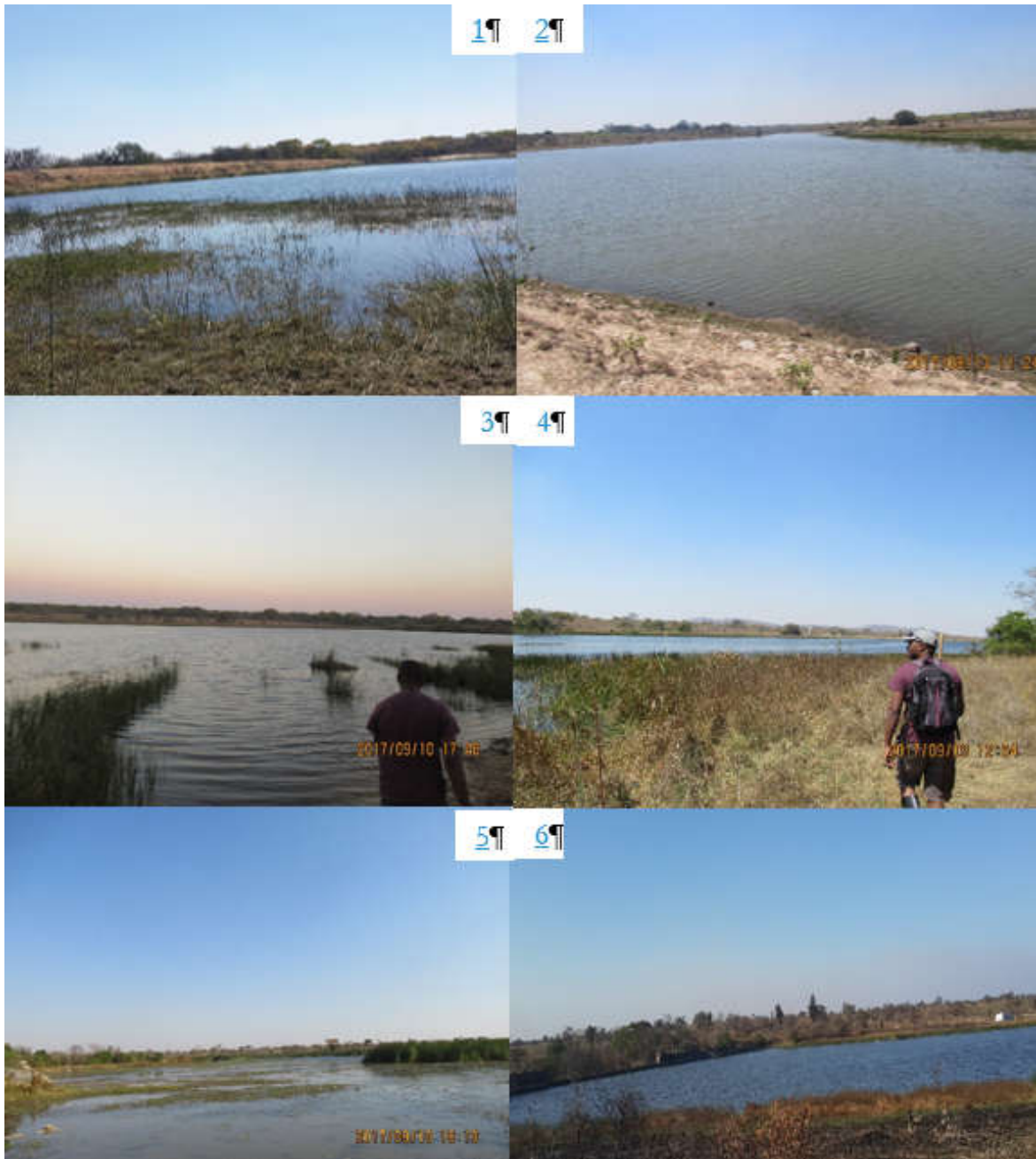


Figure 3-2. Location of all the reservoirs that formed the in-situ dataset

3.2. In-situ data set

The in-situ dataset consisted of twenty-one small reservoirs. The data were collected between the 8th and 21st of September 2017 by walking around the perimeter of each reservoir and registering multiple points using a hand-held Garmin eTrex 30x GPS (3-5 m accuracy) unit to map the outline. The methodology used followed the procedure from Cecchi (2009), which was also successfully applied in most research on small reservoirs (Grin, 2014; Annor et al., 2009, Sawunyama, 2005, Liebe, 2002) for obtaining a ground dataset. All the reservoirs had earth embankments except for Lucilla Poort, Maguma and Mtebekwe, which were constructed from concrete. Figure 3-3 (1-6) shows some views of selected reservoirs taken during the in-situ data collection.



1. Msotswane, 2. Mutorahuku, 3.Chekabana, 4. Somabula, 5. SomKhaya and 6 Ngamo

Figure 3-3. Images of selected reservoirs during in-situ data collection

Table 3-1. Full list of reservoirs that formed the in-situ dataset

Name	Area of location	Usage	Catchment
Council	Rural	livestock	Sanyati
Ingwe	Rural	livestock	Sanyati
Shagari	Rural	livestock	Gwaai
Zaloba	Former commercial farm	livestock	Sanyati
Maguma_wier	Rural	Irrigation gardens, livestock	Sanyati
Mtebekwe wier	Rural/former commercial	Irrigation/livestock	Runde
Msoro	Rural	Brickmaking, livestock	Gwaai
Vunku	Old small scale rural farms	livestock	Gwaai
Hovelands	Educational Institution farm	Commercial	Sanyati
SoNgwenya	Rural	Gardens, brick making	Gwaai
St Patricks	Rural	Irrigation, livestock, fishing	Sanyati
Somkhaya	Rural	Livestock, brickmaking	Gwaai
Mkoba	Rural	Irrigation, livestock, fishing	Gwaai
Chekabana	Old smallscale rural farming zone	Livestock/ fishing	Gwaai
Fletcher	Semi_urban/peri urban	Peri_urban, recreational for educational institutions	Runde
Mutorahuku	Rural	Irrigation & livestock	Sanyati
Ngwena	Former commercial farm	Irrigation, smallscale	Runde
Musotswane	Half rural/half government training institution	Primary water supply & livestock ,fishing	Sanyati
Somabula	Former commercial farming	Primary water supply	Runde
Lucillia Poort	Mining	Mining & Irrigation	Runde
Ngamo	City of Gweru reservoir	Livestock & wildlife	Gwaai

3.3. Procedure of recording vertices

Vertices were recorded as either waypoints or tracks on the GPS receiver depending on the difficulty of accessing the shoreline. Some of the reservoirs have intensive grass and reeds growing on their edges thereby inhibiting accurate access to the shoreline from outside the reservoir. Fishermen usually create permanent tracks towards the water during fishing expeditions and these gave a way to access the shoreline and record the GPS points. In some circumstances, where the shoreline was clear, the area function of the GPS unit was used. After the fieldwork exercise, the GPS data was offloaded using EasyGPS (TopoGrafix, 2016) and then exported to Global mapper 18 (Blue Marble Geographics, 2017) to digitise into ArcGIS format polygons. Figure 3.4 shows the result of carrying out the procedure of collecting multiple points around the shoreline of the Somkhaya reservoir. It is mainly used for livestock watering and had a perimeter of 947.38 m and a surface area of 2.301 ha at time of fieldwork.

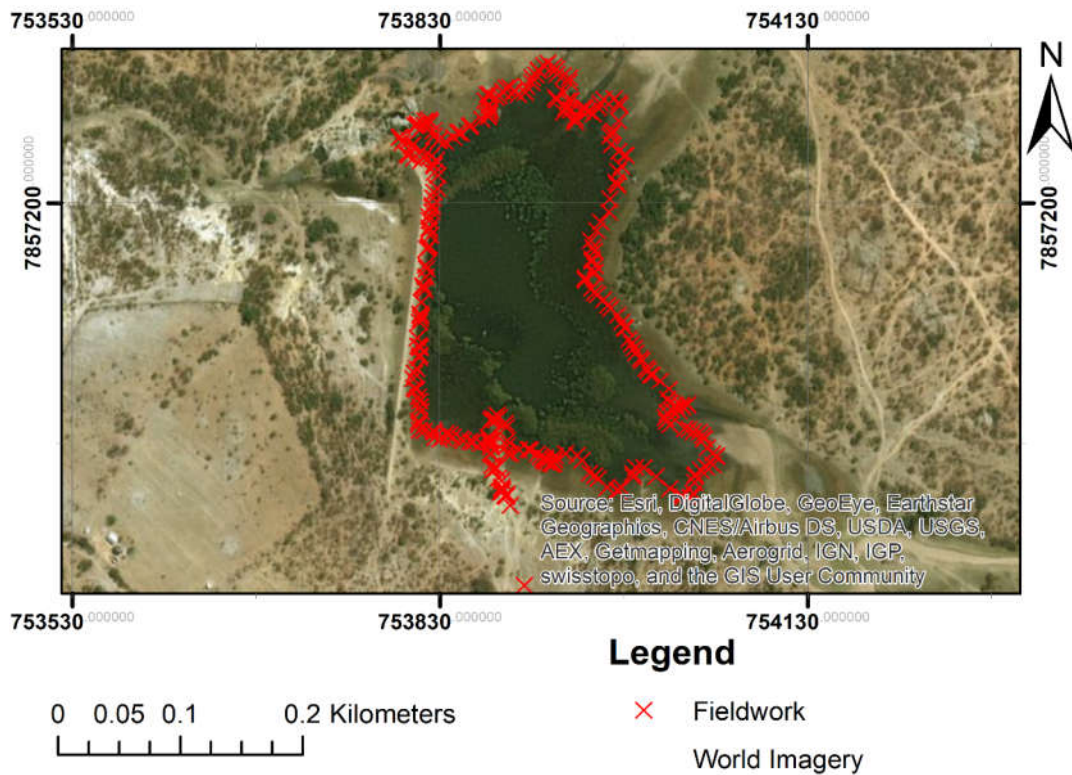


Figure 3-4. Extraction of the shoreline of the Somkhaya reservoir (12/09/2017)

3.4. Digitising the in-situ dataset

The surface areas the digitised ArcGis format polygons were simultaneously computed during the digitising process. A 10% margin of error in surface area extraction was adopted due to issues related to the accessibility of the shoreline. The data was separated into two sets and thirteen reservoirs were dropped from further analysis and are presented in Table 3.2.

Table 3-2. List of reservoirs dropped from further analysis

ID	Reservoir	Surface area ha	Remarks
2	Lucillia Poort	30.53	Mountainous. Difficult to access the shoreline at some points.
10	Somkhamba	5	Heavily silted with vegetation in the centre of the reservoir
11	St Patricks wier	3.97	Small size
12	SoNgwenya	3.4	small size
13	Hovelands	2.689	Heavy vegetation on the edges. Shoreline not easy to access.
14	Vunku	2.3	Medium dense vegetation on the edges, small size
15	Msoro	1.705	Small size
16	Mtebekwe wier	1.385	Long and narrow
17	Maguma wier	0.788	Long and very narrow
18	Zaloba	0.52	Small size
19	Shagari	0.47	Very small in size
20	Ingwe	0.388	Very small in size
21	Council	0.333	Very small in size

Eight reservoirs of different sizes were chosen for further analysis and are presented in Table 3.3.

Table 3.3. Reservoir surface area calculation for the selected reservoirs

Source: Fieldwork exercise 8-20 September 2017

ID	Reservoir	Area (Ha)	Area (m ²)	Area [-10% error] (m ²)
1	Ngamo	37.06	370632	333569
2	Somabula	21.660	216600	194940
3	Msotswane	20.240	202400	182160
4	Ngwena	10.870	108700	97830
5	Fletcher	9.540	95400	85860
6	Mutorahuku	8.990	89900	80910
7	Chekabana	7.930	79300	71370
8	Mkoba	7.620	76200	68580

4. SATELLITE IMAGERY

4.1. Sentinel-1 SAR

Sentinel-1 SAR is part of the European Copernicus program and comprises a pair (Sentinel-1A and B) of near-polar sun synchronous orbiting satellites. For Zimbabwe, Sentinel-1 SAR observations are available as in the Interferometric Wide (IW) swath mode VV and VH dual-polarisations although it potentially delivers images in HH, VV, HH+VV and VV+VH (Table 4.1) every 12 days. (Potin et al., 2016).

Table 4-1. Characteristics of Sentinel-1 SAR sensor.

Source: <https://sentinel.esa.int/web/sentinel/missions/sentinel-1/instrument-payload/resolution-swath>

Mode	Incidence Angle	Resolution	Swath width	Polarization (H-Horizontal, V-Vertical)
Stripmap	20 - 45	5 x 5 m	80 km	HH+HV, VH+VV, HH, VV
Interferometric Wide swath	29 - 46	5 x 20 m	250 km	HH+HV, VH+VV, HH, VV
Extra Wide swath	19 - 47	20 x 40 m	400 km	HH+HV, VH+VV, HH, VV
Wave	22 – 35;35 - 38	5 x 5 m	20 x 20 km	HH, VV

One hundred and thirty-three Level-1 Ground Range Detected (GRD) Sentinel-1 C-band (5.405 GHz) images collected in the Interferometric Wide swath (IW) mode were downloaded from the Sentinels Science data hub (<https://scihub.copernicus.eu/dbus/#/home>, last visited on 10 October 2017). Pre-processing of the downloaded images using the Sentinel Application Platform (SNAP) downloaded from the ESA website (<http://step.esa.int/main/download/>) was carried out using an automated processing chain constructed in graph builder. Geometric corrections, (Range Doppler shift terrain, and incidence angle normalization), and application of a 3x3 median speckle filter to reduce random noise (Amitrano et al, 2015; Liu, 2016), conversion from intensity ($m^2 m^{-2}$) to decibel (dB), mosaicking and final sub-setting to give output GeoTIFF raster images with three bands (VH, VV and Elevation) were carried out.

After the pre-processing, thirty –four subsets in GeoTIFF layer stacked raster images had 3 bands of VV, VH and Elevation and were analysis ready products. Three subset images were from the Sentinel-1 A sensor while the rest were from the Sentinel-1 B sensor. Table 4.2 shows a list of the SAR images, which are identified by the date of image acquisition.

Table 4-2. Final GeoTIFF images used for the study

	Satellite	Date
1	Sentinel-1A	25/04/2015
2	Sentinel-1A	19/02/2016
3	Sentinel-1A	28/09/2016
4	Sentinel-1B	10/10/2016
5	Sentinel-1B	22/10/2016
6	Sentinel-1B	03/11/2016
7	Sentinel-1B	15/11/2016
8	Sentinel-1B	27/11/2016
9	Sentinel-1B	09/12/2016
10	Sentinel-1B	21/12/2016
11	Sentinel-1B	02/01/2017
12	Sentinel-1B	14/01/2017
13	Sentinel-1B	26/01/2017
14	Sentinel-1B	07/02/2017
15	Sentinel-1B	19/02/2017
16	Sentinel-1B	03/03/2017
17	Sentinel-1B	15/03/2017
18	Sentinel-1B	27/03/2017
19	Sentinel-1B	08/04/2017
20	Sentinel-1B	20/04/2017
21	Sentinel-1B	02/05/2017
22	Sentinel-1B	14/05/2017
23	Sentinel-1B	26/05/2017
24	Sentinel-1B	07/06/2017
25	Sentinel-1B	19/06/2017
26	Sentinel-1B	01/07/2017
27	Sentinel-1B	13/07/2017
28	Sentinel-1B	25/07/2017
29	Sentinel-1B	06/08/2017
30	Sentinel-1B	18/08/2017
31	Sentinel-1B	30/08/2017
32	Sentinel-1B	11/09/2017
33	Sentinel-1B	23/09/2017
34	Sentinel-1B	05/10/2017

Individual Sentinel-1 SAR image bands are Grey scale, however it is possible to view them in Red, Blue and Green (RGB) representation. Figure 4-1 shows a Sentinel-1 SAR image covering the study area in RGB.

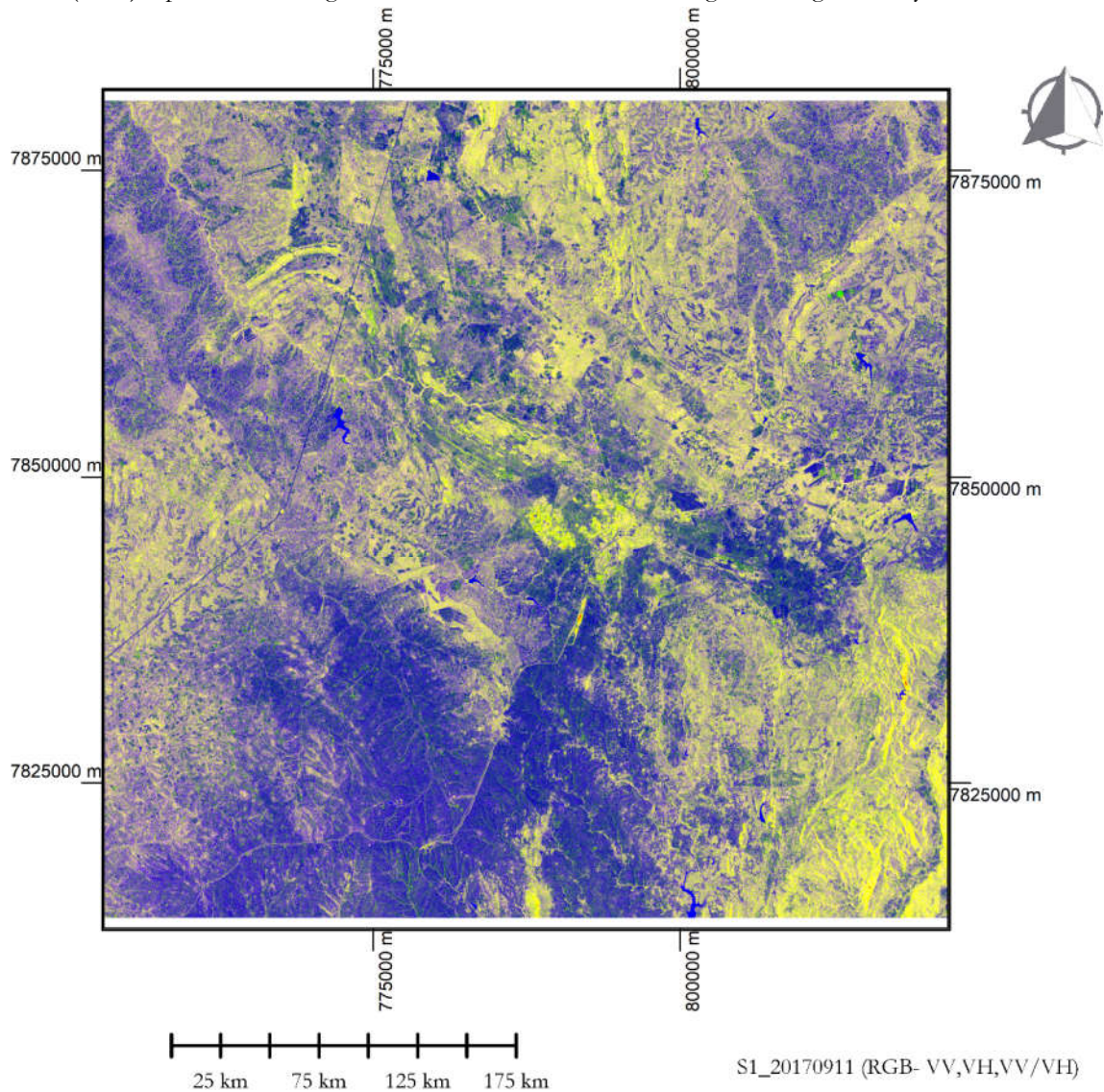


Figure 4-1. Sentinel-1 SAR image in RGB presentation

4.2. Delineation of water reservoirs using Sentinel-1 SAR

Water bodies have the lowest backscatter values against a distinctly dark tone due to specular reflection, and characteristic shape of the reservoir. Backscatter thresholding (White, Brisco, Dabboor, Schmitt, & Pratt, 2015), is the most common method of thresholding used for separating water bodies. This is a simple supervised classification method where a user selects a threshold and all pixels within the image with a backscatter will be compared against the threshold are compared (Duy, 2015).

4.3. Landsat 8 OLI

The Landsat 8 OLI was launched by NASA in February 2013 (Ko et al, 2015). It has nine 9 spectral bands (Table 4-3), 16 days temporal resolution and a spatial resolution of 30 meters for bands 1 to 7 and 9 (Barsi et al, 2014). It has a swath width covering 185 km and has been used in some studies for water body mapping and land surface monitoring in general (Wang et al, 2016).

Table 4-3. Rearranged Landsat-8 OLI spectral bands.

Source, USGS, 2015

Band No	EM zone reference	Wavelength (μm)	Resolution (m)
1	Ultra Blue (coastal/aerosol)	0.435 - 0.451	30
2	Blue	0.452 - 0.512	30
3	Green	0.533 - 0.590	30
4	Red	0.636 - 0.673	30
5	NIR	0.851 - 0.879	30
6	SWIR1	1.566 - 1.651	30
7	SWIR2	2.107 - 2.294	30
8	Panchromatic	0.503 - 0.676	15
9	Cirrus	1.363 - 1.384	30
10	TIRS1	10.60 - 11.19	100 * (30)
11	TIRS2	11.50 - 12.51	100 * (30)

Landsat-8 OLI images that were cloud free and acquired at the beginning of the dry season (or end of the rainy season) which occurs from the end of March to mid- April and early September 2016 and 2017 were downloaded from <https://glovis.usgs.gov/app>, last visited on 10 October 2017. Table 4-4 shows the list of images used in this study.

Table 4-4. List of cloud free Landsat 8 OLI images selected for the study

	Row	Path	Acquisition date
1	170	073	26/03/2016
2	170	074	26/03/2016
3	170	073	02/09/2016
5	170	074	02/09/2016
6	170	073	29/03/2017
	170	074	29/03/2017
7	170	073	05/09/2017
8	170	074	05/09/2017

Downloaded Landsat-8 OLI products are radiometrically calibrated, orthorectified, and suitable for pixel-based time series analysis (USGS, 2015, Xie et al, 2016). They were pre-processed using SNAP 5.0 toolbox through the procedures of change of geolocation (imagery was geolocated in zone 36 N), layerstacking, mosaicking, resampling and subsetting to create an output 5-band raster using bands 2,3,4,5 and 6. Index bands for NDVI, NDWI and MNDWI (Table 4-7) were created from their standard formulas using Envi+IDL 8.5 (Harris Geospatial Solutions, 2016).

One of the Landsat-8 OLI images that were used in this study is shown in Figure 4.2

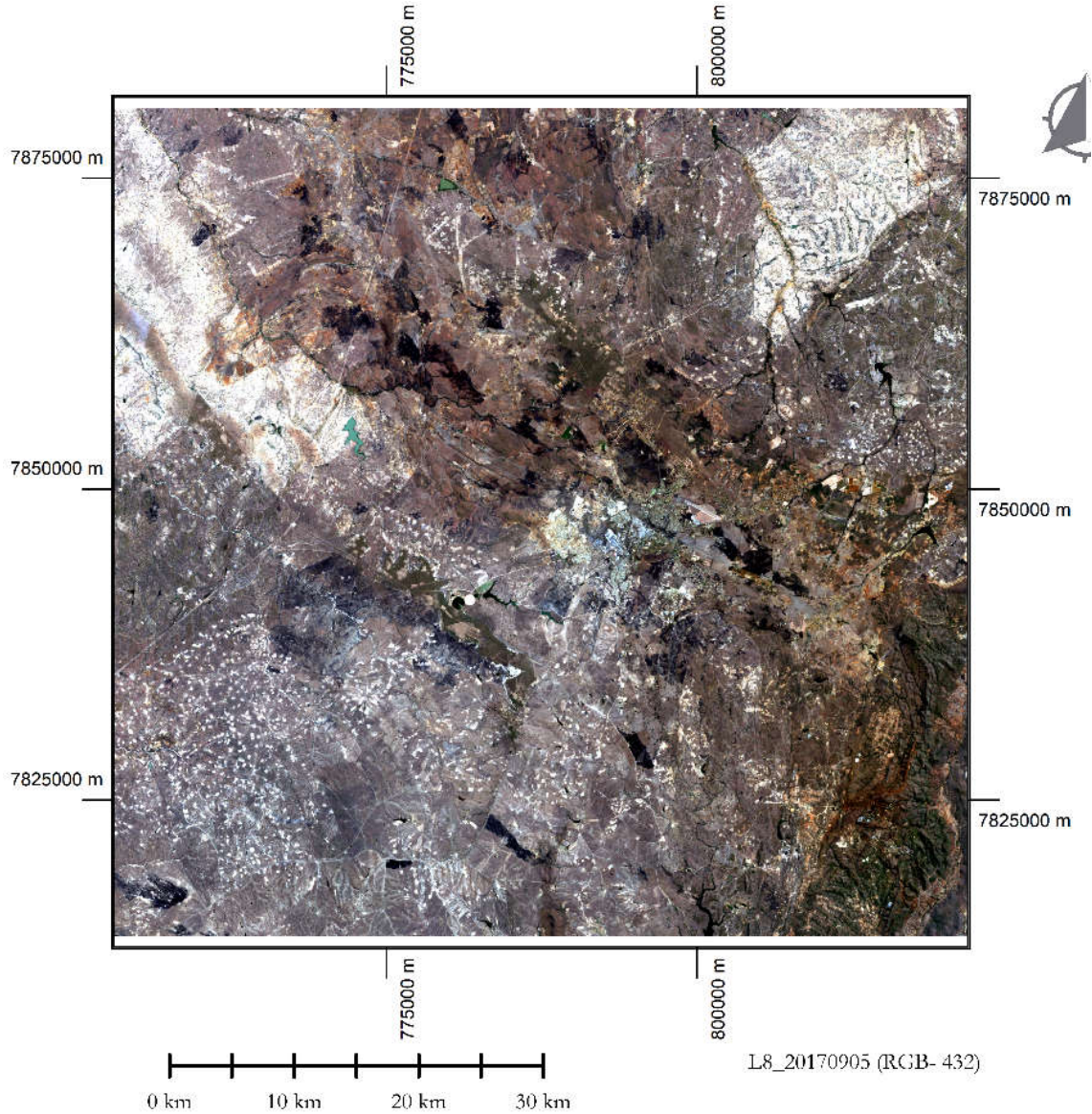


Figure 4-2. Landsat-8 OLI image in RGB presentation

4.4. Sentinel-2 MSI

Sentinel 2 MSI is a high resolution, wide-swath (290 km) multi-spectral imaging sensor carried on twin satellites (Sentinel-2A and 2B) that were launched in June 2015 and March 2017 respectively (ESA, 2015). Sentinel-2 MSI was designed to give a 12-day temporal resolution with one satellite and has the following characteristics from 13 spectral bands (Table 4.5).

Table 4-5. Rearrangement of Sentinel-2 spectral bands according to a common resolution.

Source: (ESA, 2015)

Band No	EM zone reference	Wavelength (μm)	Resolution (m)
2	Blue	0.49	10
3	Green	0.56	10
4	Red	0.665	10
8	NIR	0.842	10
5	Vegetation Red Edge	0.705	20
6	Vegetation Red Edge	0.74	20
7	Vegetation Red Edge	0.783	20
8A	Narrow NIR	0.865	20
11	SWIR1	1.61	20
12	SWIR2	2.19	20
1	Coastal aerosol	0.443	60
9	Water vapour	0.945	60
10	Cirrus	1.375	60

Sentinel-2 level 1 (L1C) scenes are provided as orthorectified, geolocated and radiometrically calibrated products in the safe format (Vanhellemont & Ruddick, 2016). Two tiles of Sentinel 2, KQU and KRU cover the study area and the list of cloud free images acquired at the end of the wet season and timing of fieldwork are listed in Table 4.6.

Table 4-6. List of cloud free Sentinel-2 MSI images available for the study area

	Tile	Tile	Acquisition date
1	170	KQU	26/03/2016
2	170	KRU	26/03/2016
3	170	KQU	17/04/2016
5	170	KRU	17/04/2016
6	170	KQU	02/04/2017
	170	KRU	02/04/2017
7	170	KQU	09/09/2017
8	170	KRU	09/09/2017

Sentinel 2 images were pre-processed using the SNAP 5.0 toolbox and bands 2, 3, 4, 8 and 11 were of interest. Band 11 of Sentinel-2 has a spatial resolution of 20 m while the rest are 10 m. The fusion of bands methodology described in Wang et al., (2016), was used to match band 11 with bands 2, 3, 4 and 8. A layer stacking of the five bands to create a mosaic was done using cropping and export tools (Appendix-1 shows the metadata from a processed image). in Global mapper (Blue Marble Geographics, 2017). The resulting subsets were loaded into ENVI 5.3 + IDL 8.5 (Harris Geospatial Solutions, 2016) to create a further 3 bands using optical water indices.

An example of the Sentinel-2 MSI images that were used in this study is shown in Figure 4.3

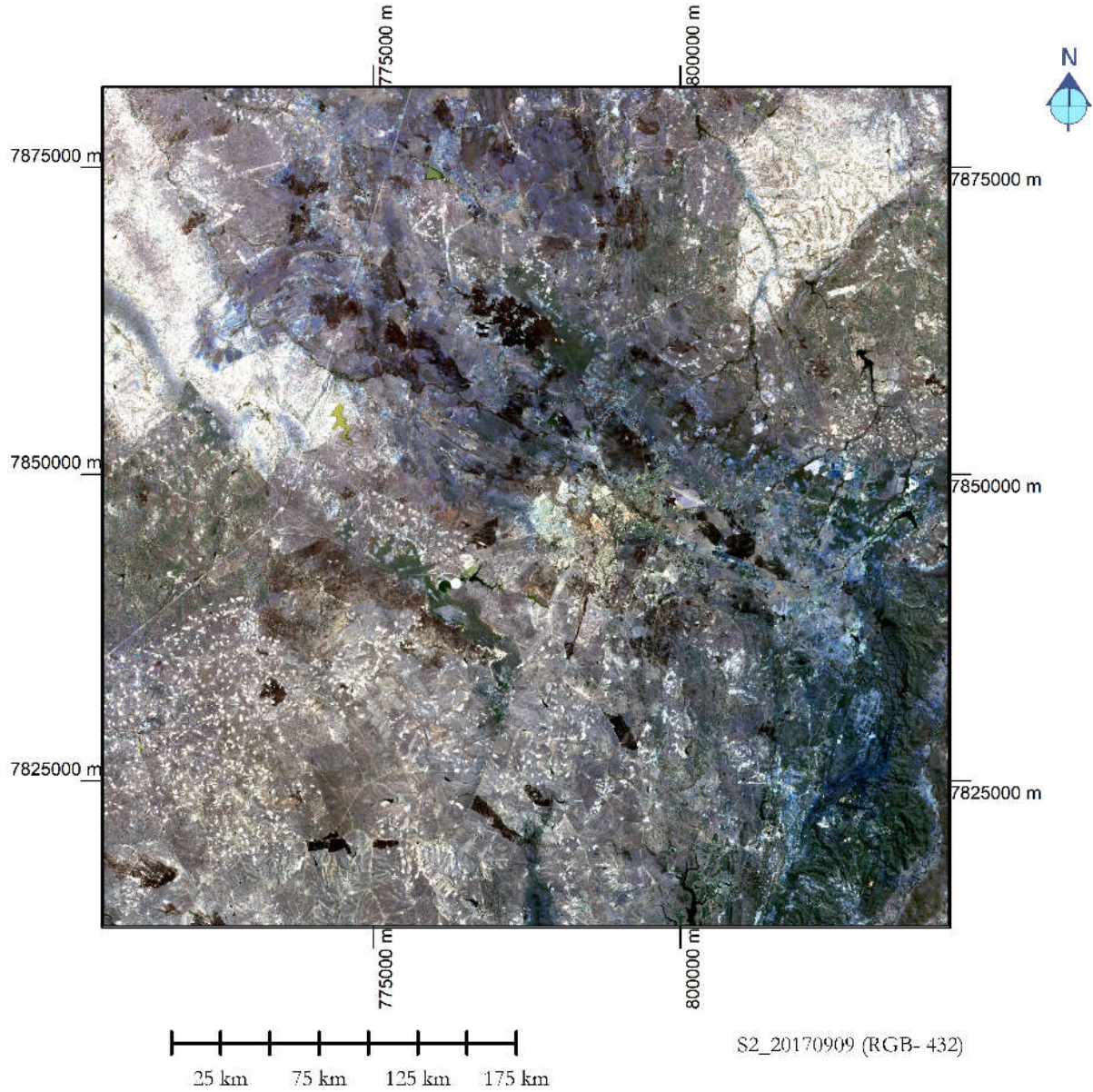


Figure 4-3. Sentinel-2 MSI image in RGB representation

5 METHODS

5.1. Masking of water bodies using optical imagery

The water indices of NDVI, NDWI and MNDWI bands were created from the expressions shown in table 5.1 because the two sensors have different band combinations; therefore band math expressions for water indices are different. Table 5.1 shows the expressions that were used

Table 5-1. Calculated water indices, their formulae and applicability to each sensor

Index	Formulae	Landsat 8	Sentinel-2
NDVI	$(NIR - Red)/(NIR + Red)$	$\frac{B5-B4}{B5+B4}$	$\frac{B8-B4}{B8+B4}$
NDWI	$(Green - NIR)/(Green + NIR)$	$\frac{B3-B5}{B3+B5}$	$\frac{B3-B8}{B3+B8}$
MNDWI	$(Green - SWIR1)/(Green + SWIR1)$	$\frac{B3-B6}{B3+B6}$	$\frac{B3-B11}{B3+B11}$

To separate water bodies and other classes, single band water masks were created from water indices from both optical datasets. They consisted of either water (1) in black or land, which was white in colour (0). It was observed that there was a different range of pixel values for each water body, image and sensor; therefore, it was necessary to establish a threshold value. A scan of the edges and the smallest portions of water bodies while observing pixel values across all the indices at the indices at the same spot was used to pick a random minimum initial value. Trial and error, using band math expressions was used until an acceptable clear separation between land and water was achieved. Equations 5.1-5.3 show the format of the expressions that were used.

$$\text{If } NDVI > \text{Threshold then Waterbody else Land} \quad (5.1)$$

$$\text{If } NDWI < \text{Threshold then Waterbody else Land} \quad (5.2)$$

$$\text{If } MNDWI < \text{Threshold then Waterbody else Land} \quad (5.3)$$

The results of the water body masking process were saved as GeoTIFF images and visually compared for their efficiency in separating land and water bodies. Figure 5.1 shows images of water body masks created from a Landsat OLI image.

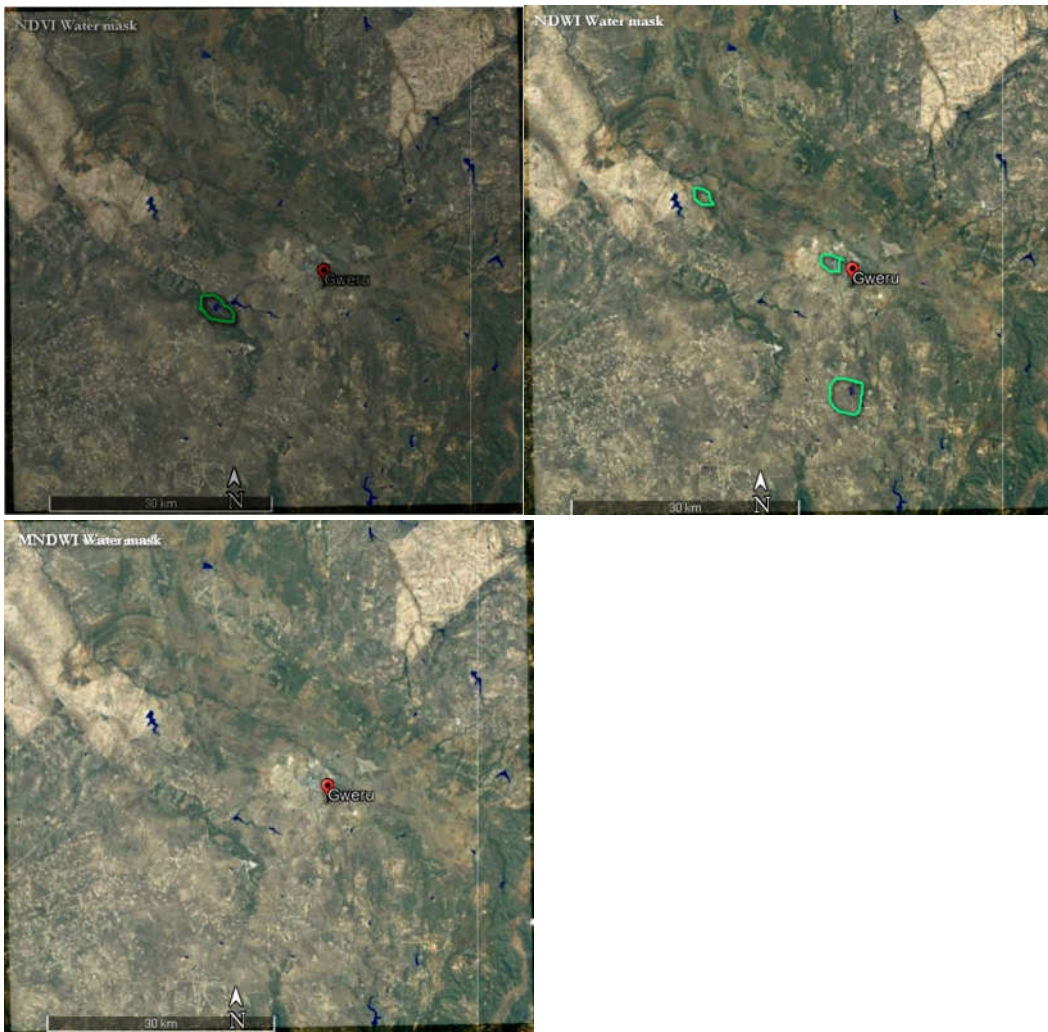


Figure 5-1. Masking of water bodies on a Landsat-8 image

Figure 5-1 shows the different water masks derived from thresholding on a Landsat-8 image. Green markings on the NDVI and NDWI show those instances of misclassification. Agricultural land was classified as water in the NDVI, while the NDWI had issues with the built up areas. MNDWI gave a better separation compared to the other 2.

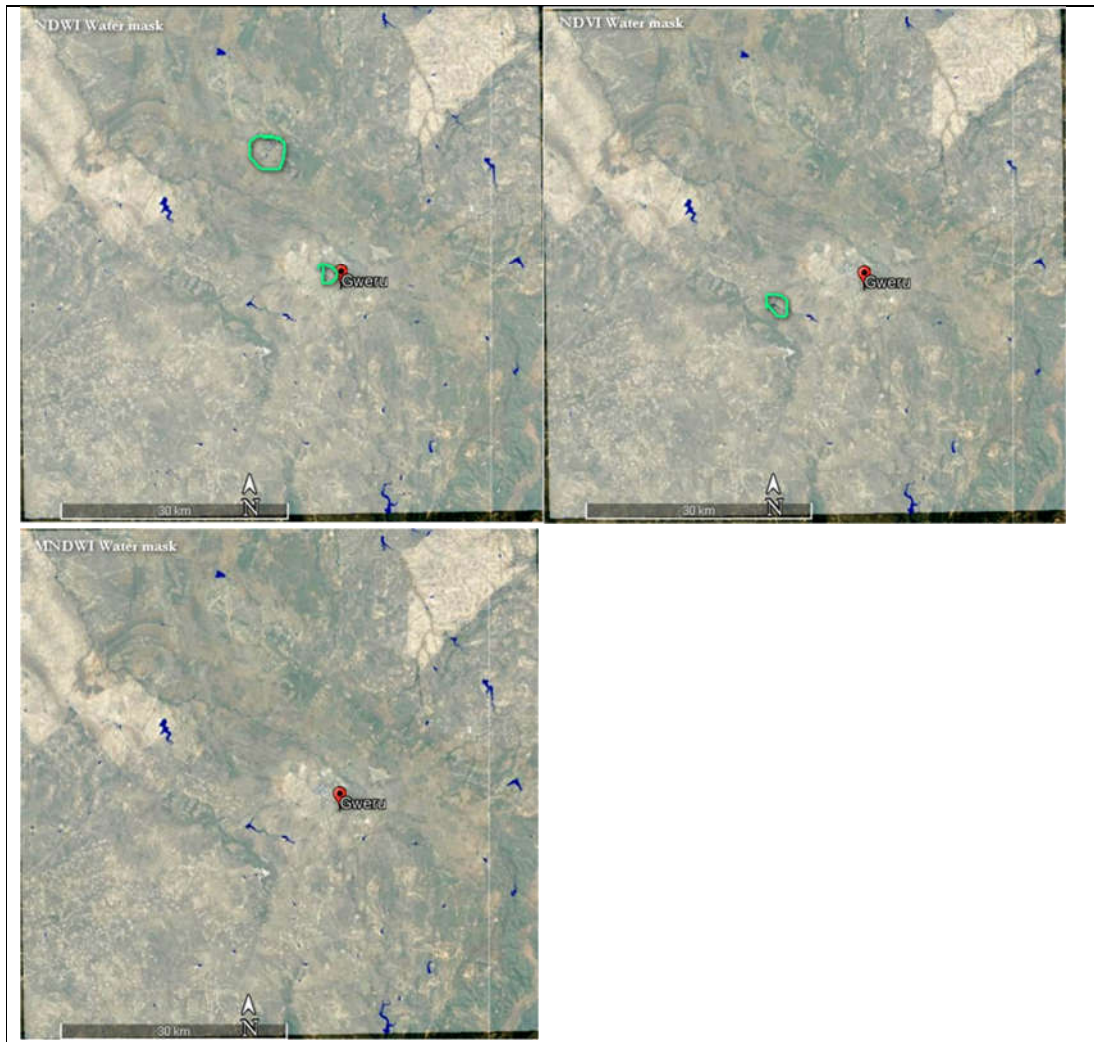


Figure 5-2. Masking of water bodies on a Sentinel-2 image

In Figure 5-2, water masks derived from a Sentinel-2 image show the same pattern as Landsat-8, however the NDVI index had problems separating built up areas as well. The water masking indicated that MNDWI performed better than NDVI and NDWI in the separation of land and water bodies in the study area, and was therefore adopted for use. Differences were observed in thresholds between images and sensors which made it necessary to threshold individual images differently as recommended by Clement, Kilsby, & Moore, (2017). Table 5.1 shows the different thresholds used for generating the MNDWI water body used for this study.

Table 5-2. Thresholds applied to the different images

Image	Threshold
S2_20170909	>0.012
S2_20160417	>0.01
L8_20170402	>0.002
L8_20170905	>0.52

5.2. Accuracy assessment and threshold determination

A calibration exercise using the September 2017 remote sensing datasets acquired during the fieldwork period was carried out. There were no images acquired on the same day, reasonable matching was however done to ensure a reasonable comparison. Table 5-2 shows the matching of September 2017 Sentinel-1, Sentinel-2 and Landsat 8 images used in the calibration and accuracy assessment.

Table 5-3. Matching of September 2017 remote sensing datasets for calibration and accuracy assessment

Sentinel-2	Landsat-8	Sentinel-1
2017.09.09	2017.09.05	2017.09.11

The MNDWI water masks were combined with Sentinel-1 SAR images to form a new 4-band raster using ENVI 5.3. The new images were saved as ENVI standard and exported to SNAP 5.0 for production of combined water body maps using different thresholds. Thresholds [VH (-21, -22, -23, -24, and -25) and VV (-16, -17, -18, -19 and -20)] were decided upon after analysing backscatter values on water bodies of different sizes for each respective σ VV or σ VH band image. Band math expressions of the format shown in Equations 5.3 and 5.4 were used to achieve the separation.

$$\text{If } \sigma \text{ VH} < (\text{backscatter value}) \text{ and } \text{MNDWI} == \text{Waterbody} \text{ then } \text{Waterbody} \text{ else Land} \quad (5.3)$$

$$\text{If } \sigma \text{ VV} < (\text{backscatter value}) \text{ and } \text{MNDWI} == \text{Waterbody} \text{ then } \text{Waterbody} \text{ else Land} \quad (5.4)$$

The resulting water body maps were converted to GeoTIFF format and exported into Global Mapper for extraction of water body polygons. Surface areas and perimeter values were generated simultaneously generated during the digitising process and reports in csv format generated (Appendix 3 and 4). Extracted surface area values were compared against the in-situ dataset using the metrics of Relative Mean Absolute Error (RMAE) and Relative Bias (Rbias). Equations 5.5 and 5.6 show the formulation of these metrics.

$$RMAE = \frac{1}{n} \sum \frac{|In-sit-Ext|}{|In-sit|} \quad (5.5)$$

$$Rbias = \frac{1}{n} \sum \frac{|Average In-sit-Average Ext|}{|Average In-sit|} \quad (5.6)$$

Where *In-sit* = In-situ value surface area (from fieldwork)

Ext = Extracted surface area (from satellite images)

The differences between RMAE and Rbias and the correlation between the in-situ and the extracted datasets were also computed. An accuracy analysis for surface area retrieval from remotely sensed datasets was compared against the in-situ dataset as a measure of their accuracy and reliability using average relative absolute error (RMAE). Five datasets are available for September 2017 and consist of the in-situ, Sentinel-2, Landsat-8, Sentinel-2+Sentinel-1 and Landsat-8+Sentinel-1. All extractions of surface area polygons were carried out using the raster to vector conversion tool in QGIS.

5.3. Sentinel-1 SAR time series

A time series was developed from surface area extractions from Sentinel-1 SAR images trained on the April Sentinel-2 image using *if* functions in SNAP. The same threshold was applied on the SAR images because they were acquired using the same incidence angle. Equations 5.3 and 5.4 (above) were applied on the SAR images only because the April Sentinel-2 derived water mask was used throughout. The thresholds applied for creating binary images for the MNDWI band and those used on Sentinel-1 SAR images are shown in Table 5-3.

Table 5-4. Thresholds applied on the optical and SAR images

Image	Band	Threshold
Sentinel-2 20160417	S2_MNDWI	>0.012
All Sentinel-1 images	VH	<-22dB
	VV	<-18 dB

Reservoir outlines were extracted from the new binarised VH or VH images using raster to vector conversion tools in QGIS. For those reservoirs that had detached water pixels, merging of polygons and summing up of attributes was done using geometry tools. The generated surface area extraction report was exported into a spreadsheet for analysis.

5.4. Translating Area to Volume

Developing a rating curve for each reservoir is time consuming and intensive, however it was not possible in this research. Remote sensing is not able to extract the volume therefore three basin-derived Surface area-Volume relationships based formulas developed in Zimbabwe were used instead. A comparison of the three methods was based on how best the equations represented storage. The theory behind the relationships between surface area and the depth makes assumptions that reservoirs located in the same physiographic area have almost similar shapes. The most common shape in Africa is a square pyramid diagonally cut in half (Magome et al., 2003) however, realistically multiple other shapes do exist. The formulas (Mazvimazvi et al., 2004; Mitchell, 1976; Sawunyama, 2005) have different basin specific constants and exponents that were developed for different regions within Zimbabwe. Surface area extractions for each respective Sentinel-1 SAR/Sentinel-2 trained extraction were converted to storage for each reservoir. The computed volumes were summed up and plotted against time to explain the dynamics of storage volumes from each formula. However, there was no in-situ dataset to validate which therefore made it difficult to conclude.

6 RESULTS & DISCUSSION

6.1. Identifying a suitable threshold

To identify optimum threshold values, an extraction and a comparison of σ_{VV} and σ_{VH} , derived surface areas of selected water reservoirs against the in-situ dataset was carried out using the Metrics of RBias and RMAE statistics. The initial thresholds were -16 dB for σ_{VV} and -18 for the σ_{VH} . Trial and error of incremental values was used for identifying the threshold. Table 6-1 shows the errors that were obtained from Sentinel-1 SAR trained on Landsat-8 image while Table 6-2 shows the ones from Sentinel-1 trained on Sentinel-2.

Table 6-1. Error propagation on Sentinel-1 SAR trained on Landsat-8

	VH					VV				
	-21	-22	-23	-24	-25	-16	-17	-18	-19	-20
RMAE	0.403	0.425	0.450	0.484	0.573	0.465	0.446	0.477	0.495	0.538
RBias	0.359	0.380	0.404	0.439	0.518	0.437	0.404	0.435	0.455	0.500
Correlation	0.986	0.986	0.984	0.980	0.975	0.964	0.985	0.985	0.983	0.976
RMAE-RBias	0.044	0.044	0.046	0.045	0.055	0.028	0.042	0.042	0.039	0.038
Relative absolute error (-)										
Reservoir	-21	-22	-23	-24	-25	-16	-17	-18	-19	-20
Mkoba	0.500	0.510	0.553	0.572	0.671	0.464	0.488	0.519	0.541	0.573
Chekabana	0.459	0.482	0.506	0.532	0.618	0.496	0.507	0.544	0.575	0.629
Mutorahuku	0.146	0.180	0.220	0.258	0.425	0.210	0.206	0.265	0.283	0.353
Fletcher	0.441	0.452	0.473	0.510	0.601	0.463	0.512	0.512	0.515	0.564
Ngwena	0.738	0.763	0.778	0.808	0.848	0.738	0.752	0.775	0.785	0.804
Msotswane	0.347	0.382	0.404	0.485	0.613	0.577	0.426	0.474	0.494	0.549
Somabula	0.288	0.312	0.310	0.330	0.386	0.452	0.337	0.359	0.367	0.374
Ngamo	0.306	0.320	0.351	0.377	0.421	0.318	0.338	0.367	0.398	0.458

Table 6.2. Error propagation on Sentinel-1 SAR image trained on Sentinel-2

	VH					VV				
	-21	-22	-23	-24	-25	-16	-17	-18	-19	-20
RMAE	0.329	0.367	0.359	0.469	0.569	0.396	0.420	0.441	0.477	0.519
RBias	0.276	0.315	0.309	0.423	0.510	0.342	0.367	0.389	0.431	0.478
Correlation	0.990	0.991	0.990	0.981	0.981	0.991	0.990	0.989	0.986	0.980
RMAE-RBias	0.053	0.053	0.050	0.046	0.059	0.055	0.053	0.052	0.047	0.041
Relative absolute error (-)										
Mkoba	0.397	0.458	0.430	0.547	0.646	0.458	0.489	0.495	0.525	0.550
Chekabana	0.420	0.445	0.449	0.469	0.657	0.486	0.511	0.548	0.580	0.630
Mutorahuku	0.122	0.198	0.164	0.331	0.460	0.228	0.252	0.301	0.347	0.395
Fletcher	0.432	0.452	0.458	0.559	0.654	0.484	0.492	0.506	0.537	0.574
Ngwena	0.587	0.599	0.596	0.687	0.760	0.619	0.635	0.635	0.655	0.683
Msotswane	0.313	0.347	0.343	0.527	0.594	0.396	0.431	0.465	0.512	0.560
Somabula	0.176	0.203	0.198	0.301	0.376	0.268	0.298	0.294	0.319	0.343
Ngamo	0.189	0.237	0.237	0.332	0.404	0.232	0.255	0.285	0.345	0.415

A comparison of the two datasets shows a slightly higher correlation and slightly lower error and bias when the Sentinel-2 image is used. Across both datasets, there is a decrease in error, as the value of σ_{VH} becomes smaller i.e. -21 to -22 dB. It is also the same situation with the σ_{VV} where lowering the threshold introduces more error. There is less error within larger sized reservoirs than smaller ones throughout. Figures 6.1 and 6.2 further illustrate the differences between the two polarisations.

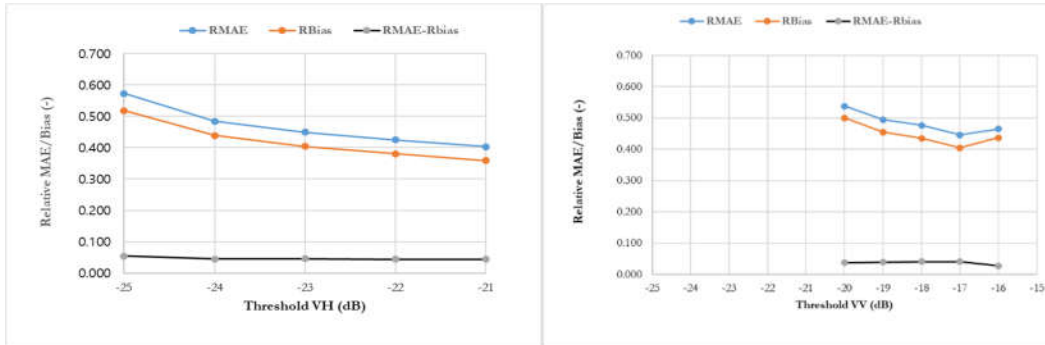


Figure 6-1. Analysis of error on the Landsat-8 image, 20170905 image

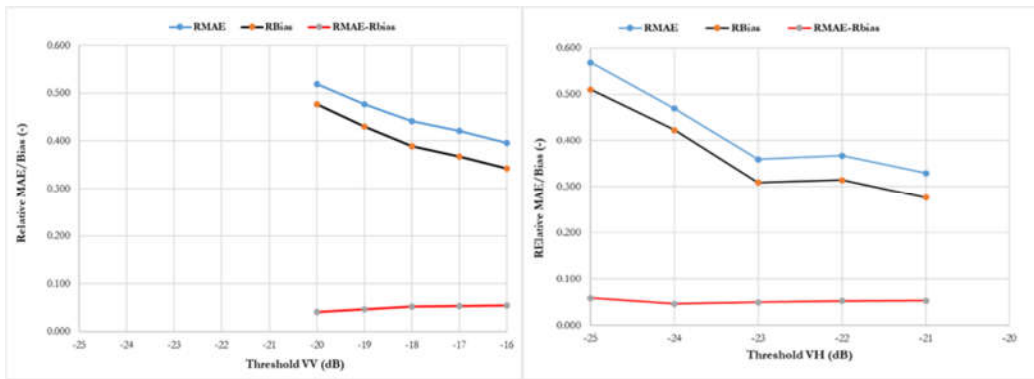


Figure 6-2. Analysis of error on the Sentinel-2, 20170909 image

Overall, there is a very large error but a low proportion of the error consists of the bias. There is less bias for the VH compared to the VV polarisation. Somabula and Ngamo are larger reservoirs that are not under intensive usage which have high performance. However, the Mutorahuku reservoir is under intensive irrigation but performed much better than the three larger reservoirs. Mkoba is also under intensive usage but did not perform as well as Mutorahuku while Chekabana and Fletcher also performed poorly even though they are also not under serious usage. It is difficult to conclude that performance was related to usage, however the Mutorahuku reservoir had an easily accessible shoreline all round which played a big role in its performance. Using the Sentinel-2 image gives better results than the Landsat, confirming its superior resolution, although it is still difficult to draw a conclusion on which polarisation performs better.

To further explain the differences, the Ngwena reservoir which performed the worst in the analysis are compared with the best performing Mutorahuku reservoir (Tables 6.1 and 6.2) at the same thresholds of σ_{VV} and σ_{VH} to give a better indication of the best estimate of the threshold. Figures 6.3 to 6.6 show surface area extractions of the Ngwena and Mutorahuku reservoirs from different the same test thresholds for both Sentinel-2 and Landsat-8.

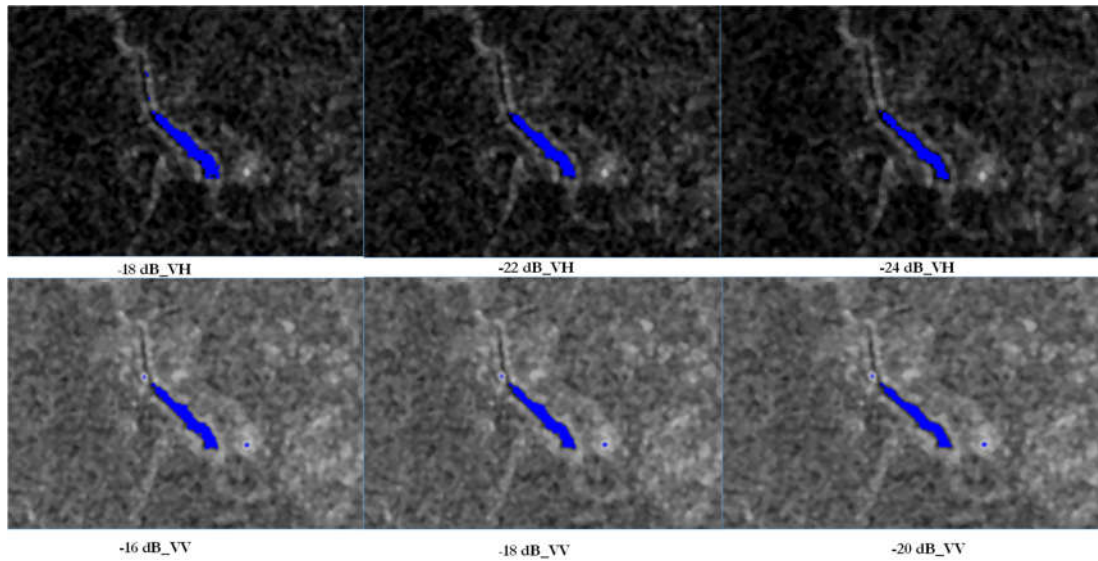


Figure 6-3. Finding the optimal threshold on Ngvena using Sentinel-1 SAR and Sentinel-2

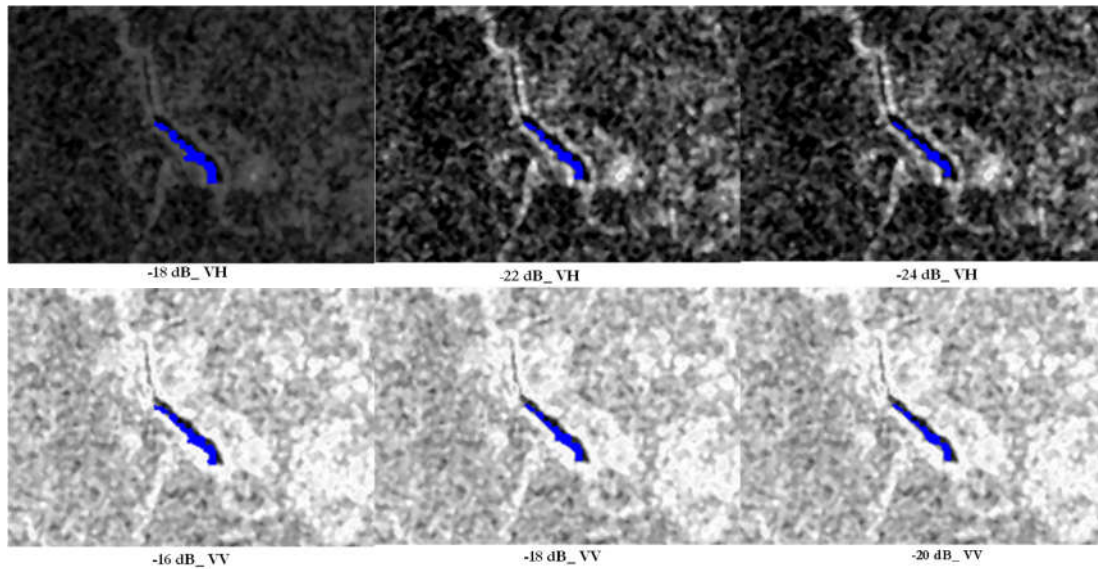


Figure 6-4. Finding the optimal threshold on Ngvena using Sentinel-1 SAR on Landsat-8

Figures 6-3 and 6-4 show the extractions of the Ingwe reservoir trained on Sentinel-2 and Landsat-8 respectively. Detected water pixels are shown in blue while the darker tone shows land. On Sentinel-2, there are less misclassified pixels manifesting as gaps on the edges and inside the reservoir on both illustrations compared to Landsat-8. Extractions of surface area covered by the reservoir are also higher on the σ VH threshold of -22 dB and -18 dB for σ VV respectively. On Landsat-8, all the extractions of surface area using both polarisation were not very different from each other. [Appendix](#) .

Mutorahuku reservoir was the best performing in consistency in surface area extraction and error analysis. Its images are shown in Figures 6.5 and 6.6.

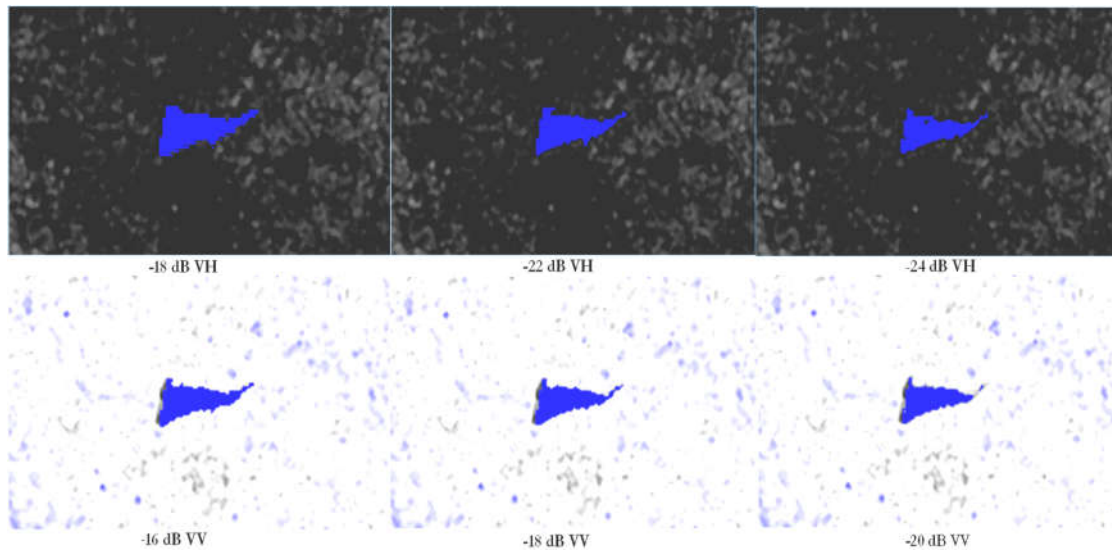


Figure 6-5. Finding the optimal threshold on Mutorahuku using Sentinel-1 SAR on Sentinel-2

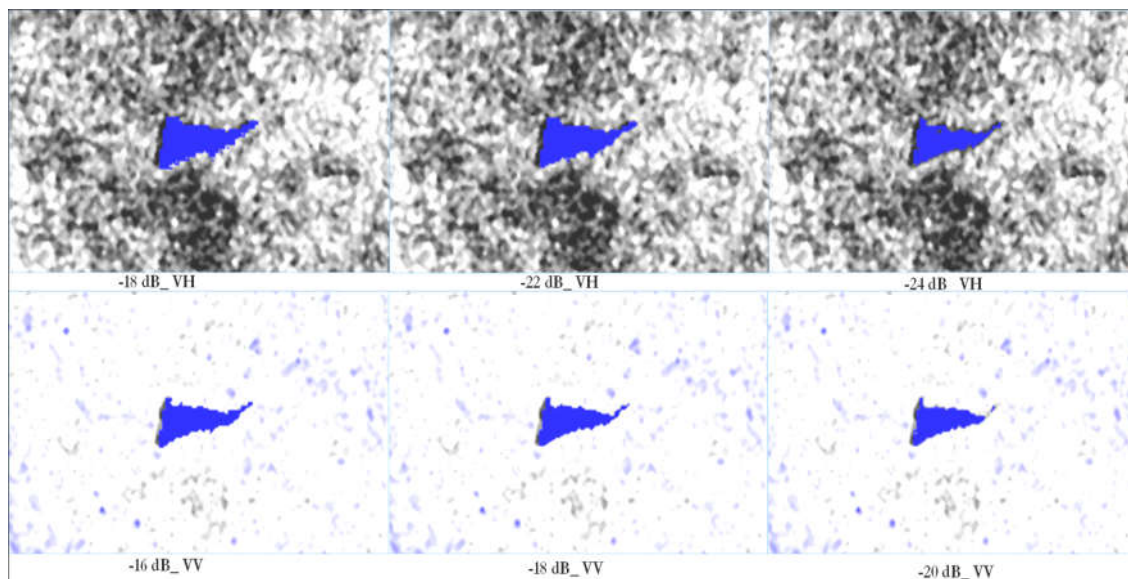


Figure 6-0. Finding the optimal threshold on Mutorahuku using Sentinel-1 SAR on Landsat-8

The extractions on Mutorahuku are relatively consistent with each other and therefore, deviating from the thresholds of -18 dB for VV results in some loss of water pixels. Loss of water pixels is mainly from the edges on the VH polarisation when σ_{VH} is high and from inside the reservoir when it is lower than -22 dB. Visually, the retrievals are not very different and the figures above helped to take a decision on the optimum thresholds from the five that were tested for each polarisation. Overall, thresholds of -18 dB for the VV and -22 dB for the VH were decided based on the visualisations because they indicated optimal extractions on both reservoirs which. Both Sentinel-1 SAR polarisations are sensitive to water bodies, but in a different manner (Pham-duc, Prigent, & Aires, 2017) although the VH polarisation seems to be more stable and has better discriminative capabilities. Santoro et al., (2015) mentioned that during in unfavourable windy conditions, higher backscatter values are returned to the sensor and are therefore registered as noise on the images. In this case, the location and orientation of the reservoir will play a role in interfering with backscatter.

6.6. Time series

A time series was constructed from surface area extractions from both VV and VH polarisations using all available Sentinel-1 SAR images covering the period 28/09/2016 to 05/10/2017. The high resolution Sentinel-2 mask for 02/04/2017 was used because it has a resolution that matches Sentinel-1 SAR and performs better than Landsat-8. The April 2 image represents the full supply capacity of all reservoirs as a straight line. The fluctuations of surface area over time captured by Sentinel-1 SAR are shown in Figure 6.7.

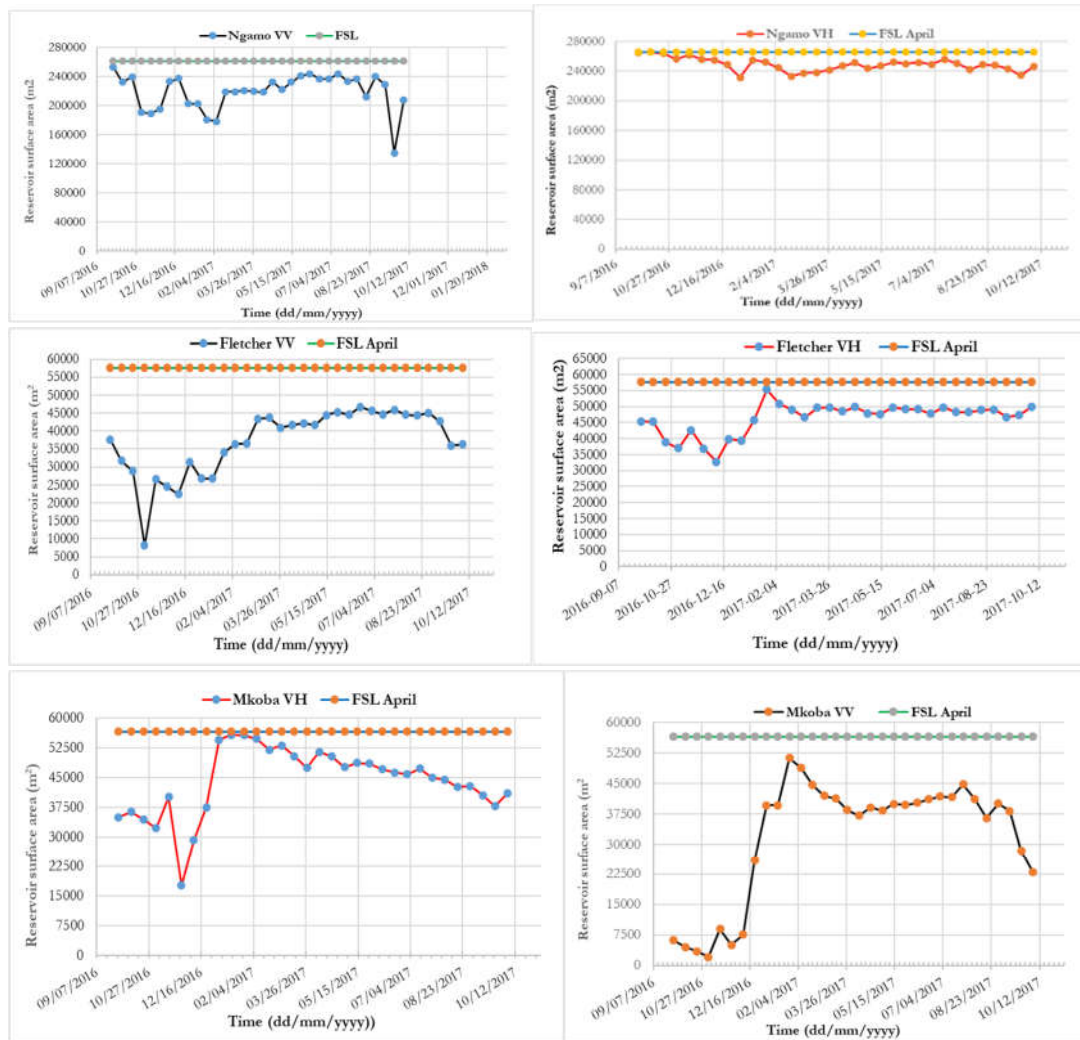


Figure 6-7. Time series of extracted surface area from selected reservoirs

Time series analyses on selected reservoirs revealed some inherent noise from data collected in 2016 data on both polarisations but more pronounced on the VV. This could be attributed to the recalibration of the sensor. Lower pixel counts were observed in smaller and elongated reservoirs such as Ngwenya and Mkoba. According to Clement et al, (2017), both VH and VV are subject to classification errors, but VH produces a wider range of backscatter values leading to chances of values of lower backscatter being found in non-water classes as well. Identification of a suitable threshold becomes difficult (Martinis et al., 2015). VH is however suited for water body detection (Duy, 2015) while the VV is more suited to flood detection as concurred by Clement et al, (2017). Research carried out using Radarsat 2 suggest that the co-polarised HH and cross polarised HV give better extractions (Bolanos et al., 2016). Pham-Duc et al.,(2017) encourage combining the different polarisations to improve the accuracy. Across all the reservoirs disturbances were pronounced on VV polarised images indicative of the effects of surface roughness, possible effects of geometry and

orientation of the sensor on the dissemination of the SAR signal (Purkis & Klemas, 2011). The full storage line (FSL) is consistently higher than the extractions. The pattern of filling and emptying capture elements of seasonality. Filling up starts from late November until around April. The larger reservoirs Somabula, Musotswane and Ngamo are more consistent with Ngamo almost registering very little change. Shape of a reservoir has some influence on backscatter because reservoirs that are long and elongated and have a lower capacity such as Ngwena and Mkoba performed poorly. While Ngamo which has a similar shape was stable. Somabula is wide and narrows gradually and performed fairly well compared to Chekabana which is almost similar in shape but has a lower capacity. Usage should play an important role in the dynamics of a reservoir, however Musotswane performed best even though it is under heavy usage from irrigation same as Mkoba. Fletcher is mainly used for recreational irrigation, and therefore it is not expected to fluctuate much.

To further illustrate the effects of physiographic parameters, extracted polygons of the Ngwena reservoir were compared at the same scale (Figure 6.8).

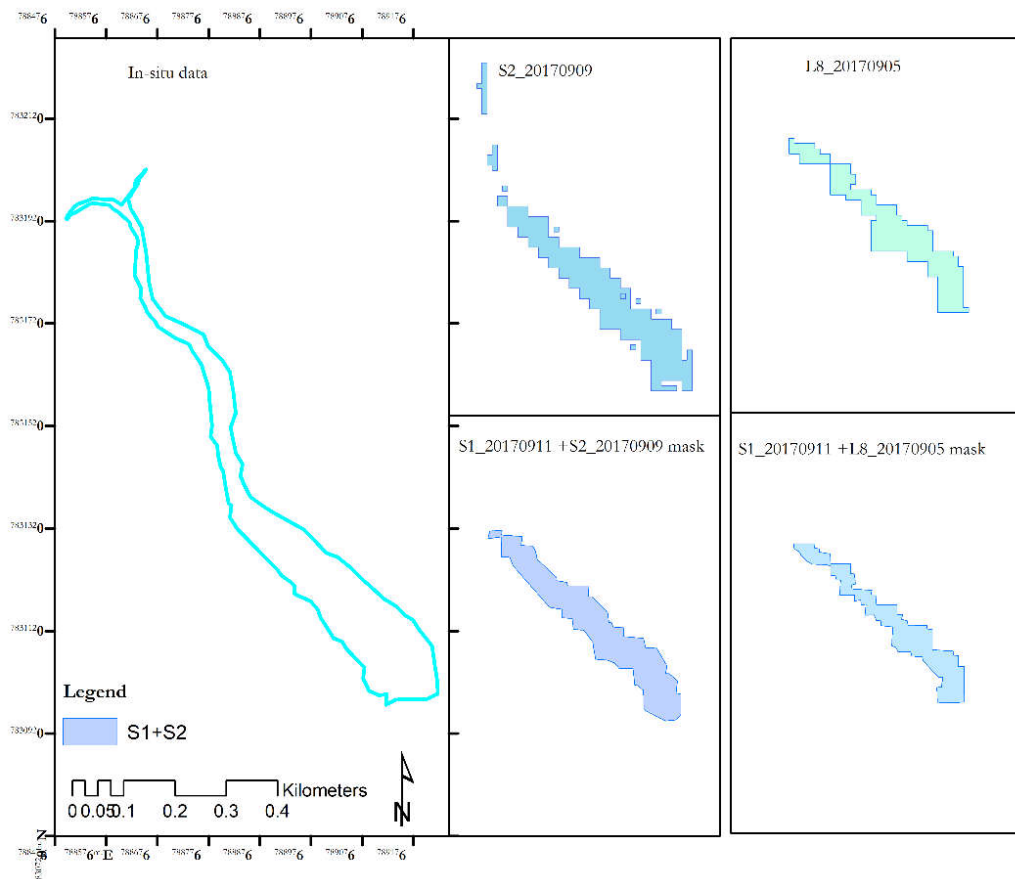


Figure 6-8. Surface area extractions on the Ngwena reservoir using different datasets

The lower section of the river was not read by any (only partially on Sentinel-2) of the remotely sensed datasets which imply that SAR alone can never be better than optical data on its own.

6.7. Accuracy of retrievals

A comparison of extractions from the different remote sensing datasets against the in-situ data collected during fieldwork was done and results are shown in Table 6.2.

Table 6-3 Surface area retrievals from the different datasets used in the study

Reservoir	In-situ	S2_20170909	L8_20170905	S2_S1-20170911	L8_S1-20170912
Extracted surface area (m ²)					
Ngwena	68852	33508	22300	28747	17018
Mkoba	68580	51488	38700	37194	33617
Chekabana	71370	47350	36800	39612	36965
Fletcher	85860	61655	52500	47628	47088
Mutorahuku	80910	78000	70600	64925	66364
Musotswane	182160	144114	119900	119020	112542
Somabula	194940	157339	136200	155393	134147
Ngamo	333569	284803	235400	254486	226949

An illustration of calculated relative errors and the efficiency with which each remotely sensed dataset is able to outline the surface areas of each reservoir is presented in Figure 6.3).

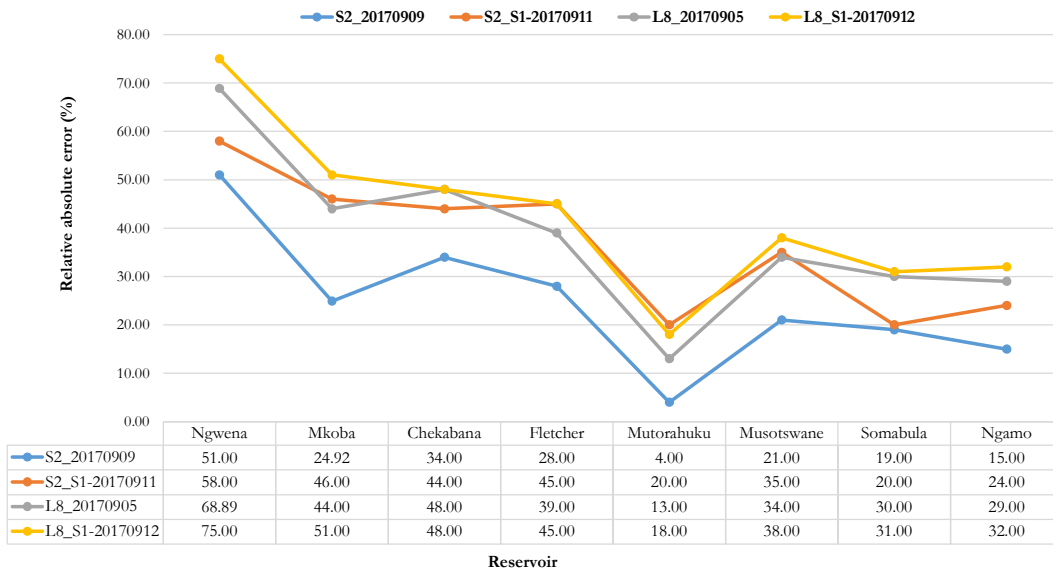


Figure 6-9. Comparison of relative errors from the different datasets

By comparison, Sentinel-2 retrievals are superior. Reservoir characteristics, location and size play a major role as well in the retrieval. Ngwena and Mutorahuku reservoirs stand out as the best and worst performing reservoirs overall. The larger reservoirs of Ngamo and Somabula have very little error associated with them and the performance in extracting the surface area is comparable. The average error for each remote sensing dataset is computed and the efficiency with which each dataset is able to extract the surface area is indicated (Table 6.2).

Table 6-4. Average relative absolute errors and inferred accuracy of each dataset

	Sentinel-2	Landsat-8	S-1+S-2 Mask	S-1+L-8 Mask
RMAE (%)	24.9	38.2	36.7	42.4
Average Accuracy (%)	75.1	61.8	63.3	57.6

Accuracy of retrievals are very low when using Landsat-8 while Sentinel-2 is much better at 75% accuracy. Sentinel-1 SAR in this is 63% accurate.

6.8. From surface area to storage

Translating the surface area to capacity was achieved by converting extracted surface areas from the VH-polarisation using the three formulas developed in Zimbabwe (Mitchell, 1976; Mazvimavi et al, 2004; Sawunyama et al, 2006). The three formula use different units and were standardised to a common unit (10^3 m^3). The computed dataset across all 32 available images was averaged to capture total storage across all reservoirs per method. The derived dataset was plotted against time of image acquisitions and is illustrated in Figure 6-10.

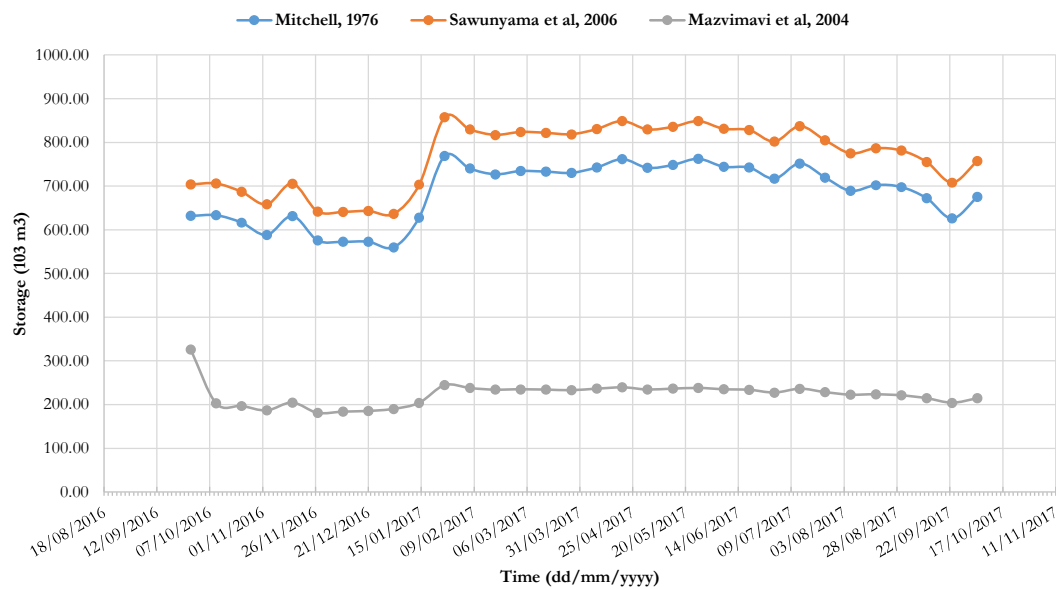


Figure 6-10. Fluctuations in storage in selected reservoirs

The results reflect consistent underestimation by the Mazvimavi et al, 2004 formula which makes it weakly incomparable to the other methods. Data from 2016 is still noisy just like in the time series, with characteristic lower values. There is an increase in storage as shown by Mitchell, 1976 and the Sawunyama et al, 2006 formulas between January and February 2017, which coincides with the peak of a normal rainfall season. Storage slightly decreases around early March and steadily increase towards the end of the rainfall season in April. There is another uncharacteristic increase in storage in August but a general trend in lower storage, which starts picking up at the last image of the series on 05/10/2017.

7. CONCLUSIONS, LIMITATIONS & RECOMMENDATIONS

7.1. Conclusions

The major objective of this study was to monitor dynamics of surface areas of small multi-purpose reservoirs not covered by institutional monitoring frameworks. Remote sensed data from a series of Sentinel-1 SAR images was used in combination with optical datasets from Sentinel-2 and Landsat-8 to extract the surface area occupied by water bodies per image acquisition based on backscatter readings. Additionally, a fieldwork exercise was carried out between 9 and 21 September 2017 to compile an in-situ dataset for comparison purposes with satellite retrievals.

The following conclusions were deduced with respect to each specific research question:

- i) What is the impact of reservoir size on the accuracy of the retrieval methodology?

- *What are the challenges in ground sampling?*

Fieldwork was successfully carried out between 9 and 21 September 2017. Twenty-one reservoirs of between 0.3 to 35 ha in surface area were visited to extract outlines of their shorelines using a handheld GPS and other data such as usage, condition and wall heights. Permissions and access were a challenge especially with local users for some of the selected reservoirs but were resolved. Usage of reservoirs is almost the same i.e. providing primary water usage needs for mostly rural communities although some provide water for irrigation or mining as additional usage. There were also problems with accessing the shorelines of almost all the reservoirs. Some of the reservoirs had tall grass and reeds growing around the edges of reservoirs and sometimes inside the reservoirs, which made access to the shoreline very challenging. Sometimes there was deep water under grass as well. One of the reservoirs was built in mountains that made it very dangerous to walk around cliffs.

The data collection method used resulted in possible over estimation of extracted surface areas despite that 10% of the surface area was removed to cater for the possible error. Walking around a reservoir is probably not the best way to obtain a ground truth dataset. A small boat would have done a better job since it will be floating in the water

- i) **Is Sentinel-1 SAR an effective data source for retrieving the surface areas of small reservoirs ?**

Generally, the use of Sentinel-1 SAR for monitoring water bodies is not common because of the difficulty of obtaining consistent results. The VV-polarisation is affected more by variations in the wind compared to the VH-polarisation. Reservoirs located in open grasslands and have elongated and narrow shape, such as Ngwena and Mkoba reservoirs, had inconsistent retrievals. However, there are significant differences between Mkoba and Ngwena because of location. Those with a wider shape and gradual narrowing performed better i.e. reservoirs Mutorahuku and Fletcher. SAR signals in the VH polarisation can be used as a reliable remote sensing estimate although due care needs to be taken into consideration because of its tendency to underestimate the surface areas. Most reservoirs have vegetation around them while one had vegetation growing within the reservoir, which affects the SAR signal and hence retrieval of the surface area. There is less noise in reservoirs with less vegetation around them as experienced with Mutorahuku reservoir, which only has vegetation on one side.

- *What is the impact of reservoir size on the accuracy of the retrieval methodology?*

Bigger sized reservoirs (>10 ha at least) in surface area generally performed better than the smaller ones because they are less affected by the edge effect. Small sized reservoirs performed poorly because of challenges with vegetation on the edges and inside the reservoirs. Geometry and location seemed to play a role in the dissemination of the SAR signal. Smaller elongated reservoirs had poor retrievals than bigger reservoirs of the same shape.

- How does storage fluctuate in different sizes of reservoirs fluctuate over time and how is it related to usage?**

Storage fluctuation mainly depends on usage and other losses. However, the three larger reservoirs of Somabula, Ngamo and Musotswane are mainly in primary use and therefore are not expected to fluctuate much. Some of the small to medium sized reservoirs for instance Mkoba and Mutorahuku were mainly built for irrigation programs and are therefore subject to usage and we would therefore expect higher fluctuations for them. In the absence of in-situ data for storage, it was difficult to validate the storage capacities computed using three methods developed in Zimbabwe. However, the use of generalized volume area relationships is discouraged because small reservoirs come in different shapes and sizes and may not suit relationships developed in other basins. At the end of the day, there are too many uncertainties and errors introduced which may be difficult to quantify, therefore storage- area relationships these models should be used with caution.

7.2. Limitations

The following limitations were encountered:

- It is difficult to obtain an accurate delineation of the shoreline of a reservoir by walking around it using a handheld GPS. This is because of the grass, reeds and shrub species which grow along the shoreline and make it impossible to access in most instances. Sometimes there will be water under grass, which cannot be read by remote sensing sensors.
- Some reservoirs had reeds inside water or islands, which could not be easily delineated during fieldwork.
- One of the reservoirs was located in a mountainous area and had dangerous cliffs, which made it difficult to delineate accurately and was therefore eliminated from further analysis.
- There is a challenge obtaining weather and water related data from authorities because of either scarcity or prohibitive costs.

7.3. Recommendations

- Investigate the influence of the shape and location of a reservoir on the SAR backscatter.
- Compare the results using another SAR satellite such as RADARSAT 2 and also compare the use of the HH polarisations.
- A high resolution DEM could be useful in checking the topography in areas with small reservoirs which should give a fairly accurate estimate of the depth so as to support remotely sensed surface areas with other geometric relationships to estimate the storage.

LIST OF REFERENCES

- Amitrano, D., di Martino, G., Iodice, A., Mitidieri, F., Papa, M. N., Riccio, D., & Ruello, G. (2014). Sentinel-1 for monitoring reservoirs: A performance analysis. *Remote Sensing*, 6(11), 10676–10693. <https://doi.org/10.3390/rs61110676>
- Amitrano, D., Di Martino, G., Iodice, A., Riccio, D., & Ruello, G. (2015). A new framework for SAR multitemporal data RGB representation: Rationale and products. *IEEE Transactions on Geoscience and Remote Sensing*, 53(1), 117–133. <https://doi.org/10.1109/TGRS.2014.2318997>
- Amitrano, D., Martino, G. Di, Iodice, A., Riccio, D., & Ruello, G. (2017). Small Reservoirs Extraction in Semiarid Regions Using Multitemporal Synthetic Aperture Radar Images. *IEEE Journal of Selected Topics in Applied Earth Observations and Remote Sensing*, 1–11. <https://doi.org/10.1109/JSTARS.2017.2692959>
- Andreini, M., Schuetz, T., Senzanje, A., Rodriguez, L., Andah, W., Cecchi, P., ... Liebe, J. (2009). *CPWF Project Number 46 Report: Small Multi-Purpose Reservoir Ensemble Planning Project Number PN46*. Retrieved from www.waterandfood.org
- Annor, F. O., van de Giesen, N., Liebe, J., van de Zaag, P., Tilmant, A., & Odai, S. N. (2009). Delineation of small reservoirs using radar imagery in a semi-arid environment: A case study in the upper east region of Ghana. *Physics and Chemistry of the Earth*, 34(4–5), 309–315. <https://doi.org/10.1016/j.pce.2008.08.005>
- Avisse, N., Tilmant, A., François Müller, M., & Zhang, H. (2017). Monitoring small reservoirs' storage with satellite remote sensing in inaccessible areas. *Hydrology and Earth System Sciences*, 21(12), 6445–6459. <https://doi.org/10.5194/hess-21-6445-2017>
- Awange, J. ., & Kyalo Kiema, J. . (2013). Microwave Remote sensing. In J. . Awange & J. . Kyalo Kiema (Eds.), *Environmental Geoinformatics- Monitoring and management* (pp. 133–144). Berlin: Springer Verlag.
- Ballatore, T. J., Bradt, S. R., Olaka, L., Cózar, A., & Loisel, S. A. Remote Sensing of African Lakes: A Review (2014). <https://doi.org/10.1007/978-94-017-8008-7>
- Barsi, J. A., Lee, K., Kvaran, G., Markham, B. L., & Pedelty, J. A. (2014). The spectral response of the Landsat-8 operational land imager. *Remote Sensing*, 6(10), 10232–10251. <https://doi.org/10.3390/rs61010232>
- Blue Marble Geographics. (2017). Global Mapper - All-in-one GIS Software. Retrieved 16 November 2017, from <http://www.bluemarblegeo.com/products/global-mapper.php>
- Bolanos, S., Stiff, D., Brisco, B., & Pietroniro, A. (2016). Operational surface water detection and monitoring using Radarsat 2. *Remote Sensing*, 8(4). <https://doi.org/10.3390/rs8040285>
- Campbell, J. B., & Wynne, R. H. (2011). *Introduction to remote sensing* (5th ed.). New York: Guilford Press. Retrieved from <http://ezproxy.utwente.nl:2200/patron/FullRecord.aspx?p=843851>
- Cecchi, P. (2009). Small Reservoirs Toolkit. Small Reservoirs Project. Retrieved from <http://www.smallreservoirs.org/>
- Chan, Y. K., & Koo, V. C. (2008). An Introduction to Synthetic Aperture Radar (SAR). *Progress In Electromagnetics Research B*, 2(6), 27–60. <https://doi.org/10.2528/PIERB07110101>
- Chevrel, M., Courtois, M., & Weill, G. (1981). The SPOT satellite remote sensing mission. *Photogrammetric Engineering and Remote Sensing*, 47(8), 1163–1171. Retrieved from <http://adsabs.harvard.edu/abs/1981PgERS..47.1163C>

- Chimowa, M., & Nugent, C. (1988). *A fisheries GIS for Zimbabwe: An initial analysis of the numbers, distribution and size of Zimbabwe's small dams*. FAO/UNDP ZIM/88/021. Retrieved from <http://www.fao.org/docrep/field/003/AB969E/AB969E00.htm>
- Chitata, T., Mugabe, F. T., & Kashaigili, J. J. (2014). Estimation of Small Reservoir Sedimentation in Semi-Arid Southern Zimbabwe. *Journal of Water Resource and Protection*, 6(August), 1017–1028. <https://doi.org/10.4236/jwarp.2014.611096>
- Clement, M. A., Kilsby, C. G., & Moore, P. (2017). Multi-temporal synthetic aperture radar flood mapping using change detection. *Journal of Flood Risk Management*, 1–17. <https://doi.org/10.1111/jfr3.12303>
- Copernicus. (2018). Sentinel satellites. Retrieved 14 February 2018, from <http://www.copernicus.eu/main/sentinels>
- Dalu, T., Clegg, B., & Nhwatiwa, T. (2013). A study of the ichthyofauna of a small tropical reservoir, south-eastern lowveld, Zimbabwe. *African Journal of Aquatic Science*, 38(sup1), 105–113. <https://doi.org/10.2989/16085914.2013.768953>
- Donchyts, G., Schellekens, J., Winsemius, H., Eisemann, E., & van de Giesen, N. (2016). A 30 m resolution surfacewater mask including estimation of positional and thematic differences using landsat 8, SRTM and OPENStreetMap: A case study in the Murray-Darling basin, Australia. *Remote Sensing*, 8(5). <https://doi.org/10.3390/rs8050386>
- Downing, J. A. (2010). Emerging global role of small lakes and ponds: Little things mean a lot. *Limnetica*, 29(1), 9–24.
- Du, Y., Zhang, Y., Ling, F., Wang, Q., Li, W., & Li, X. (2016). Water bodies' mapping from Sentinel-2 imagery with Modified Normalized Difference Water Index at 10-m spatial resolution produced by sharpening the swir band. *Remote Sensing*, 8(4). <https://doi.org/10.3390/rs8040354>
- Duy, N. B. (2015). Automatic Detection of Surface water bodies from Sentinel-1 SAR images using Valley-Emphasis Method. *VIETNAM JOURNAL OF EARTH SCIENCES*, 37(4), 328–343. Retrieved from <http://vjs.ac.vn/index.php/jse/article/view/8298>
- Eilander, D., Annor, F. O., Iannini, L., & van de Giesen, N. (2014). Remotely sensed monitoring of small reservoir dynamics: A Bayesian approach. *Remote Sensing*, 6(2), 1191–1210. <https://doi.org/10.3390/rs6021191>
- Eilander, D. M. (2013). *Remotely sensed small reservoir monitoring: A Bayesian approach*. MSc Thesis, Delft university of technology. Retrieved from <https://repository.tudelft.nl/islandora/object/uuid:002968b0-e81b-45a3-8aee-22fc38407308/?collection=research>
- Eliasson, J. (2014). The rising pressure of global water shortages. *Nature*, 517(7532), 6–6. <https://doi.org/10.1038/517006a>
- Elsahabi, M., Negm, A., & El Tahan, Abdel Hamid, M. . (2016). Performances Evaluation of Surface Water Areas Extraction Techniques Using Landsat ETM+ Data: Case Study Aswan High Dam Lake (AHDL). *Procedia Technology*, 22, 1205–1212. <https://doi.org/10.1016/j.protcy.2016.02.001>
- ESA. (2009). Synthetic Aperture Radar Land Applications Tutorial, Part I: Background and Theory. *System*.
- ESA. (2015). SENTINEL-2 User Handbook, (1), 64. <https://doi.org/GMES-S1OP-EOPG-TN-13-0001>
- ESA. (2017a). Land Monitoring - Sentinel-1 SAR - User Guides - Sentinel Online. Retrieved 31 May 2017, from <https://sentinel.esa.int/web/sentinel/user-guides/sentinel-1-sar/applications/land-monitoring>
- ESA, E. college. (2017b). Echoes in Space: Introduction to Radar remote sensing. Retrieved 29 November

- 2017, from <https://eo-college.org/>
- FAO. (2007). *DAMS AND AGRICULTURE IN AFRICA* (Vol. FAO AQUAST). Retrieved from <http://www.fao.org/3/a-bc815e.pdf>
- Feyisa, G. L., Meilby, H., Fensholt, R., & Proud, S. R. (2014). Automated Water Extraction Index: A new technique for surface water mapping using Landsat imagery. *Remote Sensing of Environment*, *140*, 23–35. <https://doi.org/10.1016/j.rse.2013.08.029>
- Finch, J. W. (1997). Monitoring small dams in semi-arid regions using remote sensing and GIS. *Journal of Hydrology*, *195*(1–4), 335–351. [https://doi.org/10.1016/S0022-1694\(96\)03228-3](https://doi.org/10.1016/S0022-1694(96)03228-3)
- Government of Zimbabwe. (2013). *National water policy*. Harare, Zimbabwe. Retrieved from <http://www.zim.gov.zw/government-ministries/ministry-environment-water-and-climate>
- Grin, S. (2014). *Geometry and water height-area-volume curves of the reservoirs in the semiarid Madalena basin in Northeast Brazil*. BSc Project, University of Twente. Retrieved from http://essay.utwente.nl/66590/1/Grin_Sido.pdf
- Haibo, Y., Zongmin, W., Hongling, Z., & Yu, G. U. O. (2011). Water Body Extraction Methods Study Based on RS and GIS. *Procedia Environmental Sciences*, *10*, 2619–2624. <https://doi.org/10.1016/j.proenv.2011.09.407>
- Harris Geospatial Solutions. (2016). ENVI - The Leading Geospatial Analytics Software. Retrieved 27 November 2017, from <http://www.harrisgeospatial.com/SoftwareTechnology/ENVI.aspx%0Ahttp://www.harrisgeospatial.com/SoftwareandTechnology/ENVI.aspx#sarscape>
- Hayashi, M., & Van Der Kamp, G. (2000). Simple equations to represent the volume-area-depth relations of shallow wetlands in small topographic depressions. *Journal of Hydrology*, *237*(1–2), 74–85. [https://doi.org/10.1016/S0022-1694\(00\)00300-0](https://doi.org/10.1016/S0022-1694(00)00300-0)
- Hudson, N. (1998). *Field Engineering for Agricultural development*. Harare, Zimbabwe: Model publishing House.
- Hughes, D. A., Mantel, S. K., Hughes, D. A., & Muller, N. W. J. (2010). Ecological impacts of small dams on South African rivers Part 1 □ : Drivers of change – water quantity and quality Ecological impacts of small dams on South African rivers Part 1 □ : Drivers of change – water quantity and quality, *36*(APRIL), 361–370.
- Ignatius, A. (2009). *Big Water, Little Water: Identification of Small and Medium-sized Reservoirs in the Apalachicola-Chattahoochee -Flint River Basin with a Discussion of their Ecological and Hydrological Impacts*. Msc Thesis Florida State University. Accessed 10 September 2017
- Jawak, S. D., Kulkarni, K., & Luis, A. J. (2015). A Review on Extraction of Lakes from Remotely Sensed Optical Satellite Data with a Special Focus on Cryospheric Lakes. *J*, *4*(4), 196–213. <https://doi.org/10.4236/ars.2015.43016>
- Jawak, S. D., & Luis, A. J. (2015). A Rapid Extraction of Water Body Features from Antarctic Coastal Oasis Using Very High-Resolution Satellite Remote Sensing Data. *Aquatic Procedia*, *4*(Icwrcoe), 125–132. <https://doi.org/10.1016/j.aqpro.2015.02.018>
- Juuti, P., & Katko, T. (2004). *From a Few to All, Long-term Development of Water and Environmental Services in Finland*. (P. S. Juuti & T. S. Katko, Eds.). Tampere: Tampere University Press, ePublications - Verkkojulkaisut. Retrieved from <http://tampub.uta.fi/handle/10024/65766>
- Ko, B. C., Kim, H. H., & Nam, J. Y. (2015). Classification of potential water bodies using landsat 8 OLI and a combination of two boosted random forest classifiers. *Sensors (Switzerland)*, *15*(6), 13763–13777. <https://doi.org/10.3390/s150613763>

- Kumar, V., Kumar, P., Murugan, P., Annadurai, M., Red, G., Gautam, V. K., ... Annadurai, M. (2015). Assessment of Surface Water Dynamics in Bangalore Using WRI, NDWI, MNDWI, Supervised Classification and K-T Transformation. *Aquatic Procedia*, 4(Icwrcoe), 739–746. <https://doi.org/10.1016/j.aqpro.2015.02.095>
- La, S., Del, B., & Hamsom, M. (1987). Understanding the Normalized Difference Vegetation Index (Ndv). *Physical Oceanography*, (1), 2–5. <https://doi.org/10.1111/j.1365-2664.2004.00878.x>
- Lavender, A., & Lavender, S. (2016). *Practical Handbook of Remote Sensing* (1st ed.). Boca Raton, USA: CRC Press.
- Lehner, B., & Döll, P. (2004). Development and validation of a global database of lakes, reservoirs and wetlands. *Journal of Hydrology*, 296(1–4), 1–22. <https://doi.org/10.1016/j.jhydrol.2004.03.028>
- Lehner, B., Liermann, C. R., Revenga, C., Vörösmarty, C., Fekete, B., Crouzet, P., ... Wissler, D. (2011). High-resolution mapping of the world's reservoirs and dams for sustainable river-flow management. *Frontiers in Ecology and the Environment*, 9(9), 494–502. <https://doi.org/10.1890/100125>
- Li, J., & Wang, S. (2017). Mapping water bodies using SAR imagery - an application over the Spiritwood valley aquifer, Manitoba, 1–13. <https://doi.org/10.4095/300213>
- Li, W., Du, Z., Ling, F., Zhou, D., Wang, H., Gui, Y., ... Zhang, X. (2013). A comparison of land surface water mapping using the normalized difference water index from TM, ETM+ and ALI. *Remote Sensing*, 5(11). <https://doi.org/10.3390/rs5115530>
- Liebe, J. (2002). *Estimation of Water Storage Capacity and Evaporation Losses of Small Reservoirs in the Upper East Region of Ghana*. MSc Thesis, Rheinischen Friedrich-Wilhelms-Universität Bonn. Retrieved from smallreservoirsproject.org/publications
- Liebe, J. R., van de Giesen, N., Andreini, M., Walter, M. T., & Steenhuis, T. S. (2009). Determining watershed response in data poor environments with remotely sensed small reservoirs as runoff gauges. *Water Resources Research*, 45(7), 1–12. <https://doi.org/10.1029/2008WR007369>
- Lillesand, T. M., Kieffer, R. W., & Chipman, J. W. (2004). *Remote Sensing and Image Interpretation* (5th ed.). Hoboken, USA: John Wiley & Sons.
- Liu, C. (2016). *Analysis of Sentinel-1 SAR data for mapping standing water in the Twente region*. MSc Thesis. ITC, University of Twente. Retrieved from www.itc.nl/library/papers_2016/msc/wrem/cliu.pdf
- Lu, S., Ouyang, N., Wu, B., Wei, Y., & Tesemma, Z. (2013). Lake water volume calculation with time series remote-sensing images. *International Journal of Remote Sensing*, 34(22), 7962–7973. <https://doi.org/10.1080/01431161.2013.827814>
- Madry, S. (2013). Introduction and History of Space Remote Sensing. In J. N. Pelton, S. Madry, & S. Camacho-Lara (Eds.), *Handbook of Satellite Applications* (Volume 2 S, pp. 657–665). Springer Science+Business Media, LLC.
- Magome, J., Ishidaira, H., & Takeuchi, K. (2003). Method for satellite monitoring of water storage in reservoirs for efficient regional water management. *Water Resources Systems*, (2), 303–310.
- Malahlela, O. E. (2016). Inland waterbody mapping: towards improving discrimination and extraction of inland surface water features. *International Journal of Remote Sensing*, 37(19), 4574–4589. <https://doi.org/10.1080/01431161.2016.1217441>
- Mantel, S. K., Rivers-Moore, N., & Ramulifho, P. (2017). Small dams need consideration in riverscape conservation assessments. *Aquatic Conservation: Marine and Freshwater Ecosystems*, 27(4), 748–754.

<https://doi.org/10.1002/aqc.2739>

- Marshall, B. E., & Maes, M. (1994). *Small water bodies and their fisheries in southern Africa*. Food and Agriculture Organization of the United Nations. Retrieved from <ftp://193.43.36.92/FI/CDrom/aquaculture/a0844t/docrep/008/V5345E/V5345E00.htm>
- Martinis, S., Kuenzer, C., Wendleder, A., Huth, J., Twele, A., Roth, A., & Dech, S. (2015). Comparing four operational SAR-based water and flood detection approaches. *International Journal of Remote Sensing*, 36(13). <https://doi.org/10.1080/01431161.2015.1060647>
- Mazvimazvi, D., Kusangaya, S., & Williams, H. B. (2004). *Assessment of the Surface Water resources of Zimbabwe and guidelines for planning*. Harare, Zimbabwe.
- McFeeters, S. K. (1996). The use of the Normalized Difference Water Index (NDWI) in the delineation of open water features. *International Journal of Remote Sensing*, 17(7), 1425–1432. <https://doi.org/10.1080/01431169608948714>
- Meigh, J. (1995). The impact of small farm reservoirs on urban water supplies in Botswana. *Natural Resources Forum*, 19(1), 71–83. <https://doi.org/10.1111/j.1477-8947.1995.tb00594.x>
- Minchella, A. (2016). Sentinel-1 Overview. Unpublished presentation. Catapult Satellite Applications and UK Space agency. Accessed 29 November 2017
- Mitchell, T. B. (1976). The yield of an average dam in rhodesia. *The Rhodesian Engineer, Paper 179* (July 1976), 37–41.
- Mufute, N. L. (2007). *The Development of a Risk-of-Failure Evaluation Tool for Small Dams in Mzingwane Catchment*. MSc Thesis, IWRM University of Zimbabwe. Retrieved from www.waternetonline.org/download/data/download/00000083/Ngoni-Mufute.pdf
- Mugabe, F. T., Hodnett, M. G., & Senzanje, A. (2003). Opportunities for increasing productive water use from dam water: A case study from semi-arid Zimbabwe. *Agricultural Water Management*, 62(2), 149–163. [https://doi.org/10.1016/S0378-3774\(03\)00077-5](https://doi.org/10.1016/S0378-3774(03)00077-5)
- Mugandani, R., Wuta, M., Makarau, A., & Chipindu, B. (2012). Re-Cclassification of the Agro-Ecological Regions of Zimbabwe in Conformity With Climate Variability and Change. *African Crop Science Journal*, 20(S2), 361–369. <https://doi.org/10.4314/acsj.v20i2>.
- Munamati, M., & Senzanje, A. (2015). Dimensions of Stakeholder Interactions in Small Reservoir Development and Management in Zimbabwe 1, (June 2015), 1–19.
- Murwira, A., Masocha, M., Magadza, C. H. D., Owen, R., & Nhwatiwa, T. (2014). Zimbabwe-Strategy for Managing Water Quality and Protecting Water Sources, (May), 1–97.
- Natural Resources Canada. (2017). Airborne and Spaceborne Radar Systems | Natural Resources Canada. Retrieved 29 December 2017, from <http://www.nrncan.gc.ca/node/9335>
- Nebraska Department of Natural Resources. (2013). *Classification of Dams*.
- Pawson, J., McNicoll, R., Davison, C., & Hill, T. (2010). *Scoping the risk assessment process for small reservoirs*. Retrieved from www.defra.gov.uk/environ/fcd
- Payen, J., Faurès, J.-M., & Vallée, D. (2012). Small reservoirs and water storage for smallholder farming The case for a new approach. Retrieved from <https://agriknowledge.org/downloads/vm40xr62q>
- Pham-Duc, B., Prigent, C., & Aires, F. (2017). Surface water monitoring within cambodia and the

- Vietnamese Mekong Delta over a year, with Sentinel-1 SAR observations. *Water (Switzerland)*, 9(6), 1–21. <https://doi.org/10.3390/w9060366>
- Postel, S. L. (2006). Water Resources: For Our Thirsty World, Efficiency or Else. *Science*, 313(5790), 1046–1047. <https://doi.org/10.1126/science.1132334>
- Potin, P., Rosich, B., Miranda, N., & Grimont, P. (2016). Sentinel-1 Mission Status. *Procedia Computer Science*, 100, 1297–1304. <https://doi.org/10.1016/j.procs.2016.09.245>
- Purkis, S., & Klemas, V. (2011). *Remote Sensing and Environmental change*. Chichester: Wiley-Blackwell.
- Ran, L., & Lu, X. X. (2012). Delineation of reservoirs using remote sensing and their storage estimate: An example of the Yellow River basin, China. *Hydrological Processes*, 26(8), 1215–1229. <https://doi.org/10.1002/hyp.8224>
- Rodrigues, L. N., Sano, E. E., Steenhuis, T. S., & Passo, D. P. (2012). Estimation of small reservoir storage capacities with remote sensing in the Brazilian Savannah region. *Water Resources Management*, 26(4), 873–882. <https://doi.org/10.1007/s11269-011-9941-8>
- Rokni, K., Ahmad, A., Selamat, A., & Hazini, S. (2014). Water feature extraction and change detection using multitemporal landsat imagery. *Remote Sensing*, 6(5), 4173–4189. <https://doi.org/10.3390/rs6054173>
- Rokni, K., Ahmad, A., Solaimani, K., & Hazini, S. (2016). A New Approach for Detection of Surface Water Changes Based on Principal Component Analysis of Multitemporal Normalized Difference Water Index. *Journal of Coastal Research*, 318(2), 443–451. <https://doi.org/10.2112/JCOASTRES-D-14-00006.1>
- Rouse, J. W., Hass, R. H., Schell, J. A., & Deering, D. W. (1973). Monitoring vegetation systems in the great plains with ERTS. *Third Earth Resources Technology Satellite (ERTS) Symposium*, 1, 309–317. <https://doi.org/citeulike-article-id:12009708>
- Rukuni, S. (2006). *Modeling the response of small multi-purpose reservoirs to hydrology for improved rural livelihoods in the Mzingwane catchment: Limpopo Basin*. MSc Thesis, IWRM, University of Zimbabwe. Retrieved from http://www.waternetonline.ihe.nl/challengeprogram/D30_Rukuni_WEAP.pdf
- SANCOLD. (2017). Dams in General. Retrieved 18 August 2017, from <http://www.sancold.org.za/index.php/about/about-dams/dams-in-general>
- Santoro, M., Wegmuller, U., Wiesmann, A., Lamarche, C., Bontemps, S., Defourny, P., & Arino, O. (2015). Assessing Envisat ASAR and Sentinel-1 multi-temporal observations to map open water bodies. In *Proceedings of the 2015 IEEE 5th Asia-Pacific Conference on Synthetic Aperture Radar, APSAR 2015* (pp. 614–619). Marina bay sand, Singapore. <https://doi.org/10.1109/APSAR.2015.7306283>
- Sawunyama, T. (2005). *Estimation of Small Reservoir Storage Capacities in Limpopo River Basin Using Geographical Information Systems (GIS) and Remotely Sensed Surface Areas*: MSc Thesis, IWRM, University of Zimbabwe.
- Sawunyama, T. (2013). *Small farm dam capacity estimations from simple geometric relationships in support of the water use verification process in the Inkomati Water Management Area*. 2013 H09, LAHS-LAPSO-LASPEI Assembly (Vol. 362). Retrieved from <https://www.scopus.com/inward/record.uri?eid=2-s2.0-84900418692&partnerID=40&md5=2e71e3d2deb3c5406a362f3f36c6727a>
- Sawunyama, T., Senzanje, A., & Mhizha, A. (2006). Estimation of small reservoir storage capacities in Limpopo River Basin using geographical information systems (GIS) and remotely sensed surface areas: Case of Mzingwane catchment. *Physics and Chemistry of the Earth, Parts A/B/C*, 31(15–16), 935–943. <https://doi.org/10.1016/j.pce.2006.08.008>

- Sayl, K. N., Muhammad, N. S., & El-Shafie, A. (2017). Optimization of area–volume–elevation curve using GIS–SRTM method for rainwater harvesting in arid areas. *Environmental Earth Sciences*, 76(10), 368. <https://doi.org/10.1007/s12665-017-6699-1>
- Scholz, M. (2015). Water Resources and Environment. In M. Scholz (Ed.), *Proceedings of the 2015 international conference on water resources and environment* (p. 451). Beijing, China: CRC Press. <https://doi.org/978-1-138-02909-5>
- Sedlak, D. (2014). *Water 4.0: The Past, Present, and Future of the World's Most Vital Resource*. Yale University Press.
- Senzanje, A., Boelee, E., & Rusere, S. (2008). Multiple use of water and water productivity of communal small dams in the Limpopo Basin, Zimbabwe. *Irrigation and Drainage Systems*, 22(3–4), 225–237. <https://doi.org/10.1007/s10795-008-9053-7>
- Senzanje, A., & Chimbari, M. (2002). *Inventory of Small dams in Africa: A case study of Zimbabwe*. Colombo, Sri Lanka, July 2002.
- Short, N., Brisco, B., & Landry, R. (2011). Monitoring open fresh water in northern environments , using SAR imagery and FmFCE FmFCE method, 15035.
- Simmers, I. (1999). *Understanding Water in a Dry Environment: Hydrological Processes in Arid and Semi-arid Zones (Iah International Contributions to Hydrogeology, 23) | Ian Simmers | download*. Retrieved from <http://book.org/book/1007872/68d0bd>
- Sisay, A. (2016). Remote Sensing Based Water Surface Extraction and Change Detection in the Central Rift Valley Region of. *American Journal of Geographic Information System*, 5(2), 33–39. <https://doi.org/10.5923/j.ajgis.20160502.01>
- IWR Water Resources (2012) Small farm dam capacity estimations from simple Geometric relationships in support of water use verification process in the Inkomati water management area. Draft Report prepared by IWR water resources for : Inkomati Catchment Management Agency. (2012), (October), 1–57.
- Stanniland, A., & Curtin, D. (2013). An Examination of the Governmental Use of Military and Commercial Satellite Communications. In C.-L. S. Pelton J.N., Madry S. (Ed.), *Handbook of Satellite Applications*. (pp. 187–219). New York, USA: Springer New York.
- Strang, V. (2004). *The meaning of water* (1st ed.). Oxford: Berg Publishers.
- TopoGrafix. (2016). EasyGPS - FREE GPS Software for your Garmin, Magellan, or Lowrance GPS. Retrieved 26 November 2017, from <http://www.easygps.com/>
- Unganai, L. S., & Mason, S. J. (2002). Long-range predictability of Zimbabwe summer rainfall. *International Journal of Climatology*, 22(9), 1091–1103. <https://doi.org/10.1002/joc.786>
- United Nations. (2017). Water. Retrieved 14 December 2017, from <http://www.un.org/en/sections/issues-depth/water/>
- USGS. (2015). *Using the USGS Landsat 8 Product*. Retrieved from www.landsat.usgs.gov/Landsat8_Using_Product.php
- Vanhellemont, Q., & Ruddick, K. (2016). Acolite for Sentinel-2: Aquatic applications of MSI imagery. *European Space Agency, (Special Publication) ESA SP, SP-740*(May), 9–13.
- Venot, J.-P., & Hirvonen, M. (2013). Enduring Controversy: Small Reservoirs in Sub-Saharan Africa. *Society*

- Journal of Natural Resources*, 26(8), 883–897. <https://doi.org/10.1080/08941920.2012.723306>
- Wang, Q., Shi, W., Li, Z., & Atkinson, P. M. (2016). Fusion of Sentinel-2 images. *Remote Sensing of Environment*, 187, 241–252. <https://doi.org/10.1016/j.rse.2016.10.030>
- WCD. (2000). Dams and Development: A new framework for decision-making. *Current Opinion in Obstetrics & Gynecology*, Vol. 23, Issue November (2000) Pp. 58-63, 23(November), 58–63. <https://doi.org/10.1097/GCO.0b013e3283432017>
- White, L., Brisco, B., Dabboor, M., Schmitt, A., & Pratt, A. (2015). *A collection of SAR methodologies for monitoring wetlands*. *Remote Sensing* (Vol. 7). <https://doi.org/10.3390/rs70607615>
- Woodhouse, I. . (2006). *Introduction to Microwave remote sensing* (1st ed.). Boca Raton: CRC Press.
- Xie, H., Luo, X., Xu, X., Pan, H., & Tong, X. (2016). Evaluation of Landsat 8 OLI imagery for unsupervised inland water extraction. *International Journal of Remote Sensing*, 37(8), 1826–1844. <https://doi.org/10.1080/01431161.2016.1168948>
- Xu, H. (2006). Modification of normalised difference water index (NDWI) to enhance open water features in remotely sensed imagery. *International Journal of Remote Sensing*, 27(14), 3025–3033. <https://doi.org/10.1080/01431160600589179>
- Yang, X., Zhao, S., Qin, X., Zhao, N., & Liang, L. (2017). Mapping of Urban Surface Water Bodies from Sentinel-2 MSI Imagery at 10 m Resolution via NDWI-Based Image Sharpening. *Remote Sensing*, 9(6), 596. <https://doi.org/10.3390/rs9060596>
- Yang, X., & Zmuda, A. (1998). Rapid extraction of water bodies from SAR imagery assisted by InSAR DEMs. *Proceedings of SPIE - The International Society for Optical Engineering*, 3503, 73–78. <https://doi.org/10.1117/12.319460>
- Zhai, K., Wu, X., Qin, Y., & Du, P. (2015). Comparison of surface water extraction performances of different classic water indices using OLI and TM imageries in different situations. *Geo-Spatial Information Science*, 18(1), 32–42. <https://doi.org/10.1080/10095020.2015.1017911>
- Zimbabwe Parliament. Water Act, Pub. L. No. Chapter 20:24 (1998). Zimbabwe: Zimbabwe Parliament. Retrieved from www.law.co.zw
- ZINWA. (2016). Zimbabwe National Water Authority (ZINWA). Retrieved 26 July 2017, from <http://www.zinwa.co.zw/>

APPENDICES

Appendix 1. Typical retrievable metadata file for Sentinel-2 subsets from Global mapper

```

DESCRIPTION=Subset_S2_20170909.tif
UPPER LEFT X=742443.180
UPPER LEFT Y=7885429.960
LOWER RIGHT X=841823.180
LOWER RIGHT Y=7804139.960
WEST LONGITUDE=29° 18.27147' E
NORTH LATITUDE=19° 5.73188' S
EAST LONGITUDE=30° 15.77197' E
SOUTH LATITUDE=19° 50.62825' S
UL CORNER LONGITUDE=29° 18.27147' E
UL CORNER LATITUDE=19° 6.58614' S
UR CORNER LONGITUDE=30° 14.89266' E
UR CORNER LATITUDE=19° 5.73188' S
LR CORNER LONGITUDE=30° 15.77197' E
LR CORNER LATITUDE=19° 49.73855' S
LL CORNER LONGITUDE=29° 18.89599' E
LL CORNER LATITUDE=19° 50.62825' S
PROJ_DESC=UTM Zone -35 / WGS84 / meters
PROJ_DATUM=WGS84
PROJ_UNITS=meters
EPSG_CODE=EPSG:32735
COVERED AREA=807860 ha
NUM COLUMNS=9938
NUM ROWS=8129
NUM BANDS=5
COLOR BANDS=0,1,2
PIXEL WIDTH=10 meters
PIXEL HEIGHT=10 meters
BIT DEPTH=80
SAMPLE TYPE=Unsigned 16-bit Integer
PCS_CITATION=WGS 84 / UTM zone 35S
GT_CITATION=GCS_WGS_1984
PHOTOMETRIC=RGB Full-Color
BIT_DEPTH=80
SAMPLE_FORMAT=Unsigned Integer
ROWS_PER_STRIP=1
COMPRESSION=None
ORIENTATION=row 0 top, col 0 lsb
PIXEL_SCALE=( 10, 10, 1 )
TIEPOINTS=( 0.00, 0.00, 0.00 ) --> ( 742443.180, 7885429.960, 0.000 )
MODEL_TYPE=Projection Coordinate System
RASTER_TYPE=Pixel is Area

```


Appendix 2. In situ data set retrieval GPS to digitising

wkt_geom	MAP_NAME	GM_LAYER	NAME	PERIMETER	ENCLOSED_A m ²	Area_Ha
Polygon ((763519.06580859923	Total_Reservoirs	All_Reservoirs	Chekabana	1922 m	79253.50	7.93
Polygon ((767253.26518673379	Total_Reservoirs	All_Reservoirs	Msoro	664.3 m	18960.93	1.90
Polygon ((766269.49199975212	Total_Reservoirs	All_Reservoirs	Mkoba	2000 m	75794.83	7.58
Polygon ((759344.22235793073	Total_Reservoirs	All_Reservoirs	Vunku	947.38 m	23018.39	2.30
Polygon ((753783.73961161600	Total_Reservoirs	All_Reservoirs	SoNgwenya	1043 m	33865.78	3.39
Polygon ((757731.69103841914	Total_Reservoirs	All_Reservoirs	Shagari	278.88 m	4692.81	0.47
Polygon ((782371.73546598595	Total_Reservoirs	All_Reservoirs	Somabula	3816 m	216629.60	21.66
Polygon ((818043.21633277530	Total_Reservoirs	All_Reservoirs	Lucillia Poort da	7 503 m	305298.31	30.53
Polygon ((806572.96906995389	Total_Reservoirs	All_Reservoirs	Hovelands	877.67 m	26885.81	2.69
Polygon ((809132.02635974343	Total_Reservoirs	All_Reservoirs	Council	308.49 m	3333.77	0.33
Polygon ((808495.37532222457	Total_Reservoirs	All_Reservoirs	Ingwe	305.57 m	3884.47	0.39
MultiPolygon (((807777.231208	Total_Reservoirs	All_Reservoirs	Maguma_wier	795.35 m	8798.53	0.88
Polygon ((807991.09170575963	Total_Reservoirs	All_Reservoirs	Musotswane	4019 m	202430.41	20.24
Polygon ((788645.65612822095	Total_Reservoirs	All_Reservoirs	Ngwena	3000 m	76503.11	7.65
Polygon ((798584.26452169008	Total_Reservoirs	All_Reservoirs	Fletcher	1 735 m	89936.03	8.99
Polygon ((820947.06017321033	Total_Reservoirs	All_Reservoirs	Mtebekwe wier	1 973 m	13845.42	1.38
Polygon ((807961.66484514297	Total_Reservoirs	All_Reservoirs	Mutorahuku	2225 m	95402.65	9.54
Polygon ((807072.04330766550	Total_Reservoirs	All_Reservoirs	St Patricks	1 780km	47286.94	4.73
Polygon ((788177.09107151138	Total_Reservoirs	All_Reservoirs	Zaloba	335.94 m	5260.12	0.53
Polygon ((753814.91245103080	Total_Reservoirs	All_Reservoirs	Somkhaya	1324 m	52638.04	5.26
Polygon ((787910.41120598185	Total_Reservoirs	All_Reservoirs	Ngamo	8033 m	370632.20	37.06

Appendix 3. a digitising report showing the Polygons in world Knowledge text

L8-20170905_S1-20170911				
wkt_geom	NAME	LAYER	PERIMETER	ENCLOSED_A
Polygon ((753840.2370	SoNgwenya	Reservoir	494 m	12405
Polygon ((788818.7365	Ngwena	Reservoir	1270 m	22090
Polygon ((763532.5958	Chekabana	Reservoir	1297 m	38081
Polygon ((766279.9625	Mkoba	Reservoir	1445 m	40267
Polygon ((798202.2472	Fletcher	Reservoir	1359 m	50528
Polygon ((807612.8468	Mutorahuku	Reservoir	1666 m	71527
Polygon ((807091.2263	Musotswane	Reservoir	2763 m	125145
Polygon ((783318.5953	Somabula	Reservoir	2695 m	144297
Polygon ((807237.6204	Musotswane	Reservoir	2842 m	120553
Polygon ((783417.3556	Somabula	Reservoir	2758 m	139981
Polygon ((787753.3658	Ngamo	Reservoir	6328 m	235233
wkt_geom	NAME	LAYER	PERIMETER	ENCLOSED_A
Polygon ((753931.0328	SoNgwenya	Reservoir	225 m	1935
Polygon ((788821.8792	Ngwena	Reservoir	1269 m	18816
Polygon ((766284.4931	Mkoba	Reservoir	1185 m	34259
Polygon ((763532.1719	Chekabana	Reservoir	1214 m	38599
Polygon ((798228.3344	Fletcher	Reservoir	1307 m	48027
Polygon ((807608.3449	Mutorahuku	Reservoir	1686 m	69063
Polygon ((807203.0160	Musotswane	Reservoir	3029 m	118896
Polygon ((783410.4016	Somabula	Reservoir	2665 m	138749
Polygon ((787475.2125	Ngamo	Reservoir	6683 m	231558

Appendix 3. Portion of time series extractions for the VH polarisation

	28/09/2016	10/10/2016	22/10/2016	03/11/2016	15/11/2016	27/11/2016	09/12/2016
Ngwena	17400	17000	16500	15850	17800	19415	20680
Chekabana	26400	26000	24800	25100	25400	20800	23800
Mkoba	35000	36300	34400	32200	40100	17600	29200
Fletcher	45400	45300	38800	37000	42600	36900	32700
Mutorahuku	64600	63900	64000	50200	67700	60500	51800
Musotswane	69900	72100	70800	75500	71500	59268	67700
Somabula	125600	124800	121900	120500	126400	124300	118300
Ngamo	265550	265500	263600	256200	261600	255800	254969

Ngwena	21600	21600	21600	21600	21600	21600	21600
Chekabana	31300	31300	31300	31300	31300	31300	31300
Mkoba	56500	56500	56500	56500	56500	56500	56500
Fletcher	57600	57600	57600	57600	57600	57600	57600
Mutorahuku	95500	95500	95500	95500	95500	95500	95500
Musotswane	137800	137800	137800	137800	137800	137800	137800
Somabula	151600	151600	151600	151600	151600	151600	151600
Ngamo	265520	265520	265520	265520	265520	265520	265520

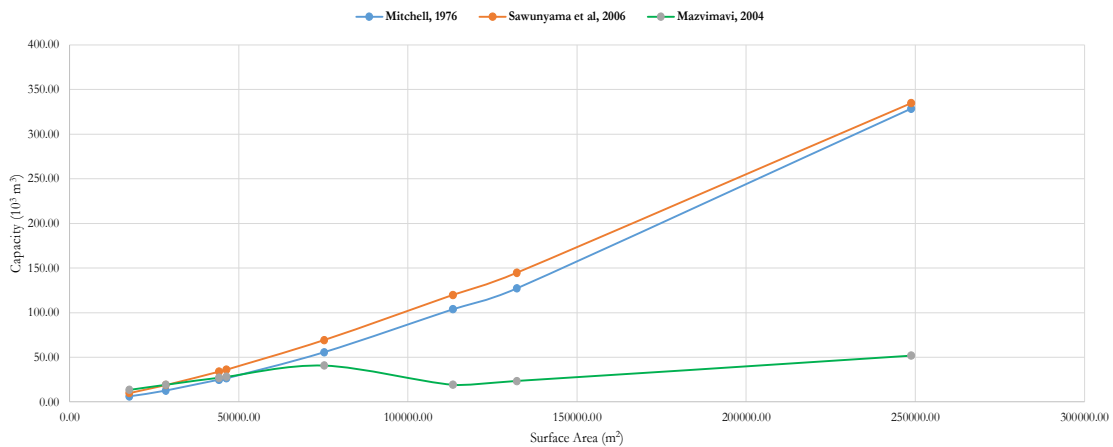
Appendix 5 Selected Time portion of the time series showing storage calculations

Mitchel	$2.646(A/10000)^{1.5} (10^3 \text{ m}^3)$							
Saunyama	$(0.023A^{1.3272})/1000 10^3\text{m}^3$							
Mazvimavi	$(7.2A^{0.77})/1000 10^3 \text{ m}^3$							
						dates		
	28/09/2016	10/10/2016	22/10/2016	03/11/2016	15/11/2016	27/11/2016	09/12/2016	
Ngwena	17400	17000	16500	15850	17800	19415	20680	
Mitchell	6.07	5.86	5.61	5.28	6.28	7.16	7.87	
Sawunyama	9.80	9.50	9.14	8.66	10.10	11.34	12.33	
Mazvimavi	13.26	13.03	12.73	12.34	13.49	14.43	15.15	
Chekabana	26400	26000	24800	25100	25400	20800	23800	
Mitchell	11.35	11.09	10.33	10.52	10.71	7.94	9.72	
Sawunyama	17.05	16.70	15.69	15.94	16.20	12.42	14.86	
Mazvimavi	18.28	18.07	17.42	17.58	17.74	15.21	16.88	
Fletcher	35000.00	36300	34400	32200	40100	17600	29200	
Mitchell	17.33	18.30	16.88	15.29	21.25	6.18	13.20	
Sawunyama	24.78	26.01	24.22	22.19	29.69	9.95	19.49	
Mazvimavi	22.71	23.36	22.41	21.30	25.22	13.38	19.76	
Mkoba	45400.00	45300	38800	37000	42600	36900	32700	
Mitchell	25.60	25.51	20.22	18.83	23.27	18.76	15.65	
Sawunyama	35.01	34.90	28.42	26.68	32.17	26.59	22.65	
Mazvimavi	27.75	27.70	24.59	23.71	26.42	23.66	21.55	

Appendix 4. Error analysis from Landsat 8 and Sentinel 1 extractions

		Satellite area (m ²)									
SAR Threshold Reservoir	In-situ surface area (m ²)	VH					VV				
		-21	-22	-23	-24	-25	-16	-17	-18	-19	-20
Mkoba	68580	41372	37194	39070	31061	24258	37139	35023	34636	32552	30838
Chekabana	71370	41420	39612	39327	37877	24459	36670	34935	32261	30009	26440
Mutorahuku	80910	71079	64925	67614	54093	43731	62494	60481	56544	52872	48919
Fletcher	85860	48759	47028	46521	37877	29723	44335	43596	42412	39791	36602
Ngwenya	71681	29572	28747	28981	22417	17197	27322	26174	26174	24705	22712
Msotswane	182160	125191	119020	119610	86133	73927	110027	103644	97474	88929	80096
Somabula	194940	160561	155393	156319	136337	121582	142701	136837	137603	132835	128162
Ngamo	333569	270571	254486	254572	222944	198670	256124	248467	238490	218434	195253

Appendix 6. Area storage relationships derived from the 3 equations



Area capacity relationships for the study area derived from existing models

Generally, all the models agree to a point between 70000 to 75000 m² in surface area. The Mazvimavi et al, 2004 shows that it does not perform very well with larger capacity reservoirs where it largely underestimates storage capacity (Mazvimavi, personal communication, February 2018). The other two models are however strongly related to each other and their competence could be validated using insitu data or other available geometric methods. Noticeably, even with the Sawunyama et al, 2004 and Mitchell, 1976 model, there is an indication of very low capacity to surface area judging from the slopes of the graphs which leads to the need of further investigation of the topography of the area using google earth based SRTM (30)

Overall, the selected reservoirs are shallow and estimated maximum depths are between 2-5 m. the relationship between the surface area capacity curves therefore points to shallower reservoirs.

It is however difficult to develop and recommend a capacity-area relationship of scientific integrity without as a high resolution DEM and depth because small errors can easily affect the reliability of estimates. There is a large variation in reservoir geometries within the study area, which subsequently implies a wide range of storage capacities for a given surface area. In reality, geometries tend to vary between catchments due to

different physiographic characteristics (Grin, 2014; Hayashi & Van Der Kamp, 2000).

Appendix 7. Time series for some reservoirs

